Jefferson Lab

Newport News, VA

Hall D Tracking and PID Review

The GlueX/HallD Central Drift Chamber

Curtis A. Meyer and Yves van Haarlem
Carnegie Mellon University

GlueX-doc-990 (version 10)

March 19, 2008

This document describes the GlueX/HallD central drift chamber. A 1.5m long straw-tube chamber that surround the GlueX target. This report provides a description of the final chamber as well as details on it construction. It also reports on completed and on-going work with a full-scale prototype chamber.

1 Introduction

Charged particle tracking in the GlueX detector is covered by two tracking systems. A cylindrical geometry around the liquid hydrogen target and a planar array in the downstream, or forward part of the detector. This document details the cylindrical system, the Central Drift Chamber (CDC). Both tracking systems are shown in the drawing of the GlueX detector in Figure 1.

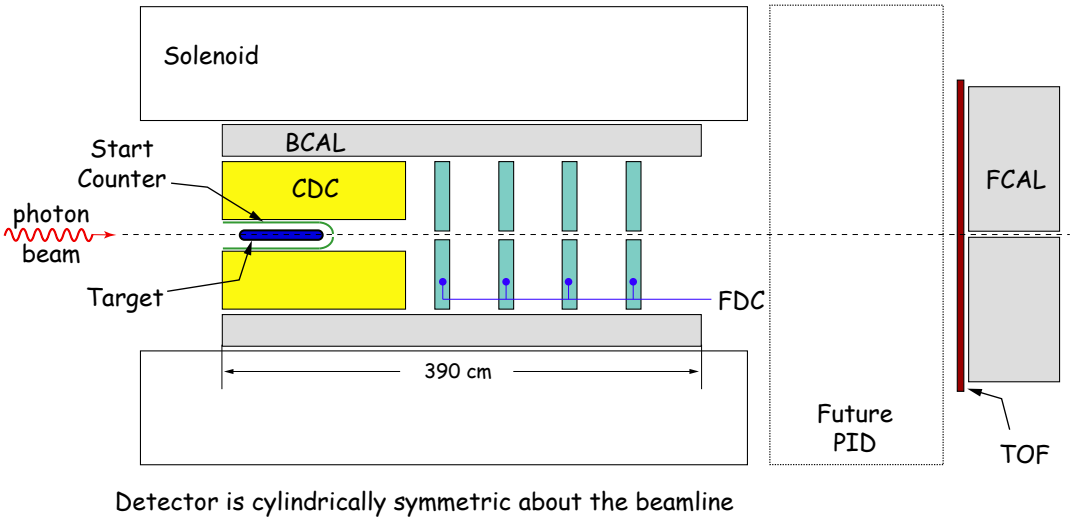

Figure 1: A cut-away view of the GlueX detector. The Central Drift Chamber (CDC) is shown as the cylindrical chamber around the target. The Forward Drift Chamber packages are shown downstream of the CDC.

The CDC will be a 1.5 m long straw-tube chamber that sits at the upstream end of the GlueX solenoid and surrounds the liquid hydrogen target. It will consist of 24 layers of 1.6 cm diameter straws that run from an inner radius of about 10 cm to an outer radius of about 54 cm. The chamber will see charged particles coming from the GlueX target with polar angles between about 6° and 165°. It will have optimal coverage from about 16° to 150° (we define optimal coverage as crossing at least 10 layers in the chamber). Tracks going more forward than about 25° will also be seen by the Forward Drift Chamber (FDC) system. Such tracks will need to travel through the downstream endplate of the CDC, so minimizing

the material in this plates is desirable.

The use of a straw-tube chamber in the central region allows us to minimize material in the tracking region. The straws can easily support the 30 to $50\,g$ of tension [1] on each of the ≈ 3100 anode wires in the chamber. In contrast, a wire-cage geometry using field wires would require supporting about $3000\,kg$ of tension between the the end plates. This would require both thick end plates as well as thick shell material at both the inner and outer radius of the chamber.

In addition to minimizing material, the straw-tube design also allows for an extremely well-defined electric field through which the ionization electrons drift. This is especially important given the $2.24\,T$ magnetic field. With straw-tubes, the time-to-radius relation can be quite accurately computed using programs such as GARFIELD [1], and is simple to implement in reconstruction. The uniform cylindrical field in a straw does not produce dead areas in the electric field. Such dead areas are are extremely difficult to model and lead to very poor position resolution for tracks passing through them. Such effects are made worse by large magnetic fields, so eliminating them with a very simple field is desirable.

In order to achieve the physics goals of GlueX [2], the CDC needs to have a position resolution perpendicular to the wires of $\approx 150\,\mu m$ ($\sigma_{r\phi}$). It also needs to be able to make some measurements along the length of the wire (σ_z) to an accuracy of $\approx 1.5\,mm$ and be able to make dE/dx measurements that will allow us to separate protons and pions below 450Mev/c [3] (above 450, particle identification will also be possible in the Barrel Calorimeter). The desired $\sigma_{r\phi}$ resolution can be obtained in the straw tube arrangement. The σ_z resolution will be achieved by placing about $\frac{1}{3}$ of the straw tubes at stereo angles of $\pm 6^\circ$ relative to the straight wires. The dE/dx will be achieved by reading out the tubes using Flash ADCs (FADCs) and then accounting for the path length in the straw [3] (see section 12.4.

In the final GlueX detector, particles which have small enough transverse momentum will be bent into circles and effectively stay within the tracking volume. In particular, many of these particles are slow protons, for those with momentum under 450 MeV/c, where the only particle identification system is the CDC. The purpose of the dE/dx measurement in the CDC is to separate these protons from similar momentum pions.

In Figure 2 we show simulations of dE/dx measurements in the CDC. The tracks are reconstructed and then the path length in each straw is computed. This is combined with energy deposited in each straw to obtain a dE/dx measurement. This has been carried out for pions kaons and protons traversing the CDC at polar angles of 90° and 15° with the results shown in Figure 2.

The arrangement of stereo layers in the CDC is dictated by two concerns. First, a measurement of the polar angle of tracks in the CDC, and second, a measurement of the z vertex position of the event. Both of these require that the first z measurement be made close to the innermost radius of the CDC. Unfortunately, for the z-measurement to be fully useful, it is necessary to have straight layers at both smaller and larger radius. This has

[1] We will use $\frac{1}{2}$ of the yield point of the sense wire and will specify that the yield be as large as possible. The quoted yields for $20\,\mu m$ Tungsten wire range from 65 to $100\,g$.

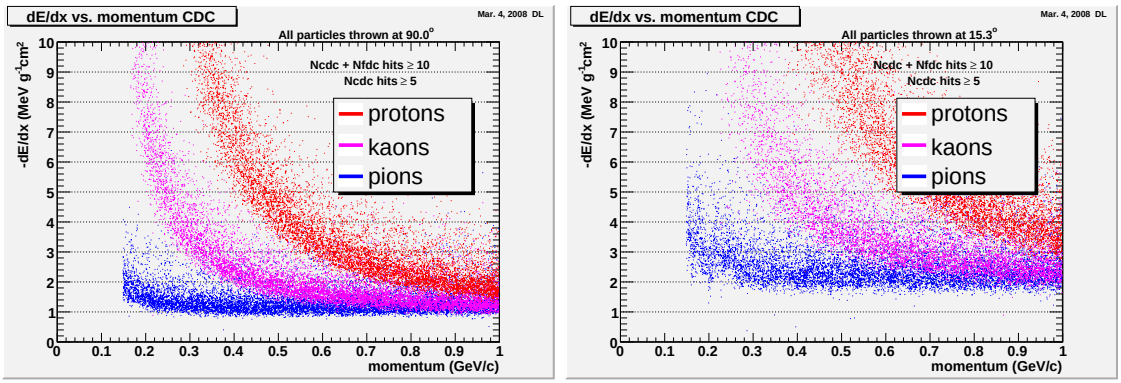

Figure 2: A simulation of the the dE/dx per straw corrected for the path length in a straw. (left) Tracks crossing at 90° and (right) tracks crossing at 15°.

led us to place the first stereo layer in layer 4 of the CDC. The second set of stereo layers should give a reasonably long lever are relative to the first, but it is also necessary that the tracks either go through both sets of stereo packages, or if the second package is missed, that at lest the first FDC package is hit. From this latter criteria, we have decided to place the second set of stereo layers ending at layer 16. We also note that up until the time that the endplates are ordered, it is possible to change the arrangement of stereo and straight wires with little or no cost or time impact on the construction schedule for the CDC.

1.1 Changes To The CDC During The Last Twelve Months

During the last twelve months, an optimization of the GlueX detector has been carried out. One crucial goal was to minimize the material in the tracking region. However, as the process evolved, problems with shadowing of the GlueX calorimeters by chamber support structures also became apparent. The result of this optimization are changes reflected throughout the GlueX detector. Here we specifically list those made for the CDC.

- The length of the active volume of the CDC has been shortened from 175 cm to 150 cm. This change is a result of the most downstream FDC element shadowing the edges of the gap between the calorimeter systems. To alleviate this, all FDC packages were moved upstream by roughly 25 cm. To maintain the total length between the two most extreme FDC packages, the CDC has been shortened by 25 cm.

- The number of layers in the CDC has decreased from 25 to 24. This is also related to the shadowing of the calorimeter. This change allows us to bring the FDC cables out from the upstream end of the magnet, rather than through the gap between the calorimeters.

- The number of channels in the CDC has decreased from 3337 to 3098. This is a result of eliminating a layer and the shortening of the chamber. The latter affects the number

of tubes in a stereo layer by decreasing the radial gap between the stereo and straight layers (see section 2.

- The downstream endplate was changed from $6\,mm$ thick Aluminum to $6\,mm$ thick carbon fiber to reduce the material in the endplate. This has reduced the number of radiation lengths of material from 6.6% to 3.7%. However, it should be noted that about one third of the carbon fiber endplate material is actually the Delrin structures which hold the tubes and wires in place.

The following descriptions reflect the above changes to the chamber and are reflected in the current set of drawings for the CDC.

2 The CDC Geometry

The GlueX CDC is shown schematically in Figure 3. The active region is $150\,cm$ long with a $0.6\,cm$ thick carbon fiber downstream endplate and a $0.9\,cm$ thick Aluminum upstream endplate. At the downstream end is a gas plenum that encapsulates a $5\,cm$ thick volume. This plenum collects the exhaust gas from the straw tubes. At the upstream end, a volume $15\,cm$ thick has been reserved for the plenum which distributes gas to the straw tubes. The upstream plenum is built out of Plexiglas to which the electronics are mounted. The downstream plenum will be a thin bag ($\approx 150\mu$m) to avoid adding material in the tracking volume. An additional $20\,cm$ of space for electronics is shown at the upstream end of the chamber from which all cables will be taken off the chamber. The inner and outer radii of the endplates are $9\,cm$ and $59.75\,cm$ respectively.

Radially, the chamber will consist of 24 layers of straw tubes arranged in rings around the beam line. The straw tubes are $0.8\,cm$ radius aluminized Kapton tubes that surround a $20\,\mu m$ diameter gold-plated Tungsten wire. Eight of the layers are placed at stereo angles of $\pm 6^{\circ}$. The straws are $100\,\mu m$ thick Kapton/tape layer with at most $5\,\mu m$ of Aluminum deposited on the inside. the tube. The number of straw tubes in each of the 24 layers are listed in Table 1. We also give the radius of each wire position at the center of the chamber and at the inside face of the two endplates. Note that for the stereo layers, the radius at the center of the chamber and that at the endplates are different leading to dead space in the chamber volume.

In order to understand the change in radius of the stereo layer, please refer to the sketch shown in Figure 4. The radius (distance from the beam line) of the wire at the endplate is given as r_e, and the distance between the endplates is given as L. We then assume that the straw is placed with a stereo angle α. The radius of the tube at the center of the chamber is given as r_c. The fact that the radius at the center of the chamber is smaller is easily seen from the fact that the wire lies in the plane that subtends the arc along the endplate. It can be shown that

$$r_c \;=\; \sqrt{r_e^2 - \left(\frac{L}{2}\tan\alpha\right)^2}\,.$$

Layer	Channels	Radius (cm) (center)	Radius (cm) (endplate)	Stereo (radians)
1	43	10.984	10.984	0.000
2	50	12.769	12.769	0.000
3	57	14.555	14.555	0.000
4	64	16.340	18.142	0.105
5	71	18.126	19.765	0.105
6	78	19.912	21.415	−0.105
7	85	21.698	23.085	−0.105
8	98	25.015	25.015	0.000
9	105	26.801	26.801	0.000
10	112	28.588	28.588	0.000
11	119	30.374	30.374	0.000
12	126	32.160	32.160	0.000
13	133	33.947	34.849	0.105
14	140	35.733	36.592	0.105
15	147	37.519	38.338	−0.105
16	154	39.306	40.088	−0.105
17	165	42.113	42.113	0.000
18	172	43.899	43.899	0.000
19	179	45.686	45.686	0.000
20	186	47.472	47.472	0.000
21	193	49.258	49.258	0.000
22	200	51.045	51.045	0.000
23	207	52.831	52.831	0.000
24	214	54.618	54.618	0.000

Table 1: This table shows the number of channels in each layer of the CDC. The radius at the center is the wire location half-way between the two endplates. The radius at the endplates is where the wire goes through the endplate. For axial layers, both radii are the same. For the stereo layers, the radius at the endplate is larger than it is at the center.

Similarly, if the wire is at a clocking angle of $\phi = 0$ at the center of the chamber, then the intersections of the wire with the endplates are at $\pm\phi_o$, where

$$\phi_o \;=\; \sin^{-1}\left(\frac{L\tan\alpha}{2r_e}\right).$$

This change in radius from the center of the chamber to the endplates creates a gap between the stereo layer and the straight layer both inside and outside the stereo. This gap becomes larger as the radius of the stereo layers is made smaller. In addition, the clocking angle ϕ_o also becomes larger as the radius at which the stereo layer is located becomes smaller.

In Figure 5 are shown where the holes for the straw tubes will be drilled in the upstream

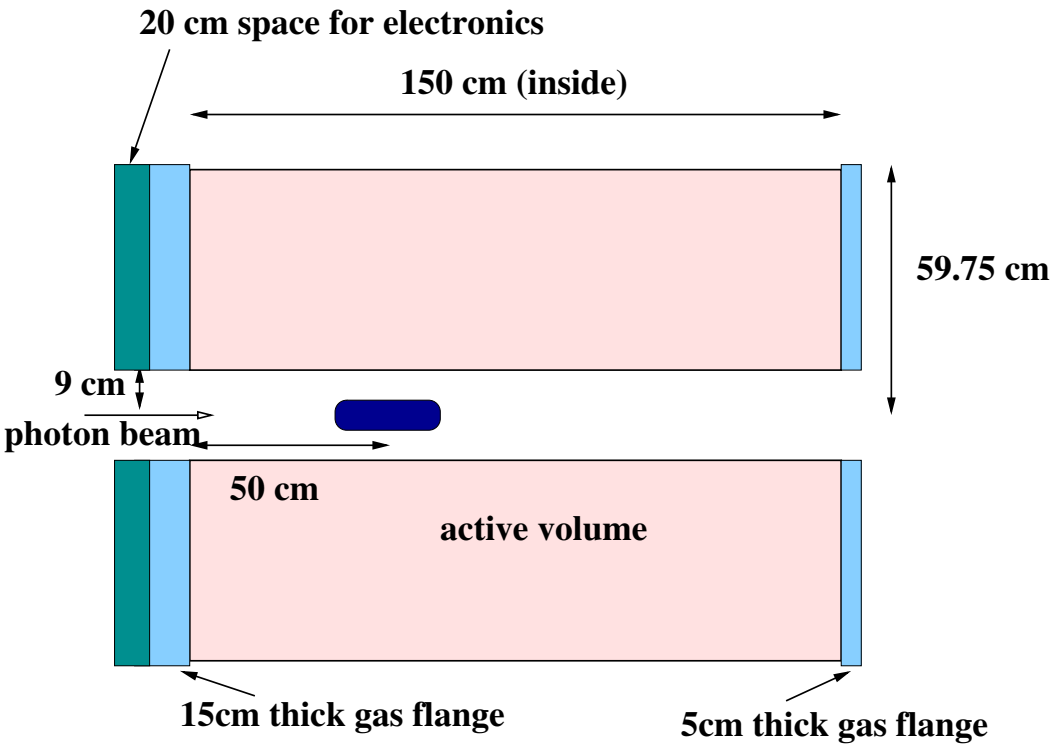

Figure 3: A side view of the CDC. The active region is 150 cm long with a 0.6 cm thick downstream endplate and a 0.9 cm thick up-stream endplate. At the downstream end is a 5 cm thick gas plenum that collects the gas from the tubes. At the upstream end a 15 cm thick plenum for distributing gas and then an additional 20 cm of space for electronics. All cables will be taken off the up-stream end of the chamber. The inner and outer radius of the endplates are 9 cm and 59.75 cm respectively.

endplate. The straight wires are shown in black, while the stereo layers are shown in color. The layout of the chamber and machining instructions are generated by a simple computer code that takes as input the inner and outer radius, as well as which layers are stereo. It then lays out the chamber such that all tubes in a given layer are touching each other, and an exact integer number of tubes fit into a layer. The in-layer touching is crucial as the tubes are glued together for structural strength and the integer number eliminates dead spaces as one goes around the beam line. The gluing is performed with a very thin epoxy at two to three points along the length of the straw.

The wires are held in place by a metallic crimp pin. The pin is inserted in a Delrin holder that has holes to allow gas flow. This in turn is inserted into a two-piece donut that is glued into the endplate. For the upstream end, the donuts are made of aluminum to provide an electrical (ground) connection between the endplate and the aluminum on the straw tube. At the downstream end, the donuts are made of Delrin to minimize the material in the chamber. Figure 6 shows schematically how the straight and stereo layers of the tubes are attached to the endplates. In particular, one should note that for the stereo layers, the

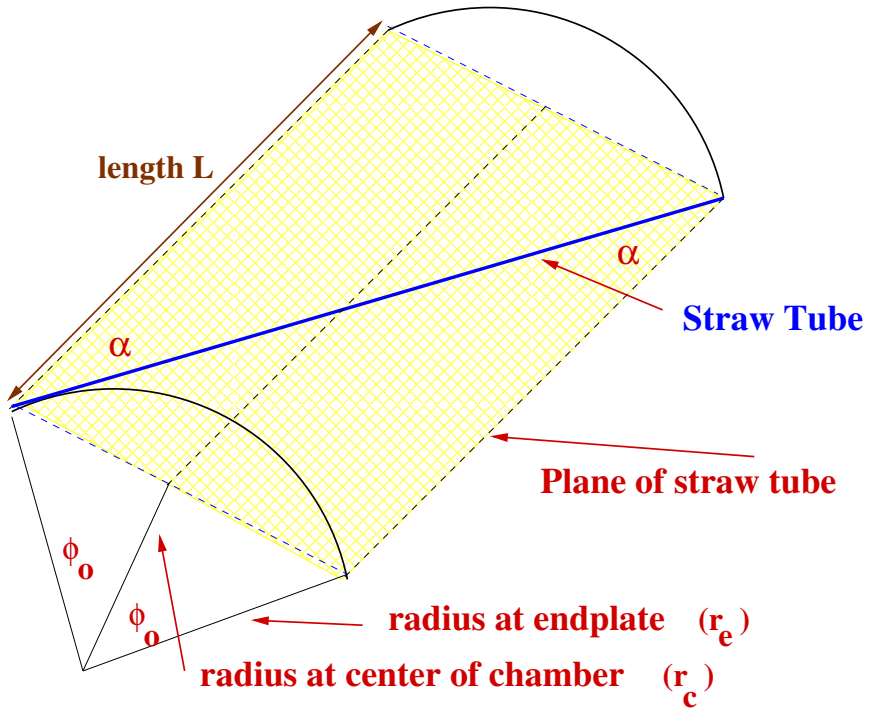

Figure 4: The placement of a stereo layer in the straw tube chamber. The radius at the center of the chamber is smaller than that at the endplates.

endplates are machined at a compound angle such that the end of the insert sits against the plate. This machining sets a minimum for the thickness of an endplate.

A problematic issue that is common with straw-tube chambers is the conductive glue joints that both hold the straws to the feed throughs, as well as the feed throughs to the chamber endplates. Careful examination of an existing straw tube chamber from the Brookhaven EVA experiment showed that all of these joints tend to develop leaks over time. In order to try to alleviate this leak problem, a detailed study of many conducting and non-conducting epoxies was carried out to see if a good glue could be found. The conclusion of this work was that the particular choice of glue did not matter. Instead, the act of inserting one part of a feed through into another part tended to scrape much of the epoxy off the contact surface. This led to a joint with many weak spots, that over a short period of time, developed leaks.

Studies have shown that the only way to guarantee a good glue connection was to develop a system in which one is certain the the glue is actually making solid contact with both surfaces. The result of this is a feed through system as shown in Figure 7. The *donut* is a small tube with a small *glue trough* machined into its perimeter. From one end of the donut, a small *glue port* is drilled from the outside to the *glue trough*. Once the donut has been inserted into the straw tube, a known amount of conducting epoxy can be injected through the *glue port* into the *glue trough*. The strength of the resulting glue joint is solid, independent of the tested epoxies. In fact several test cells have maintained several psi overpressure for several months without leaking.

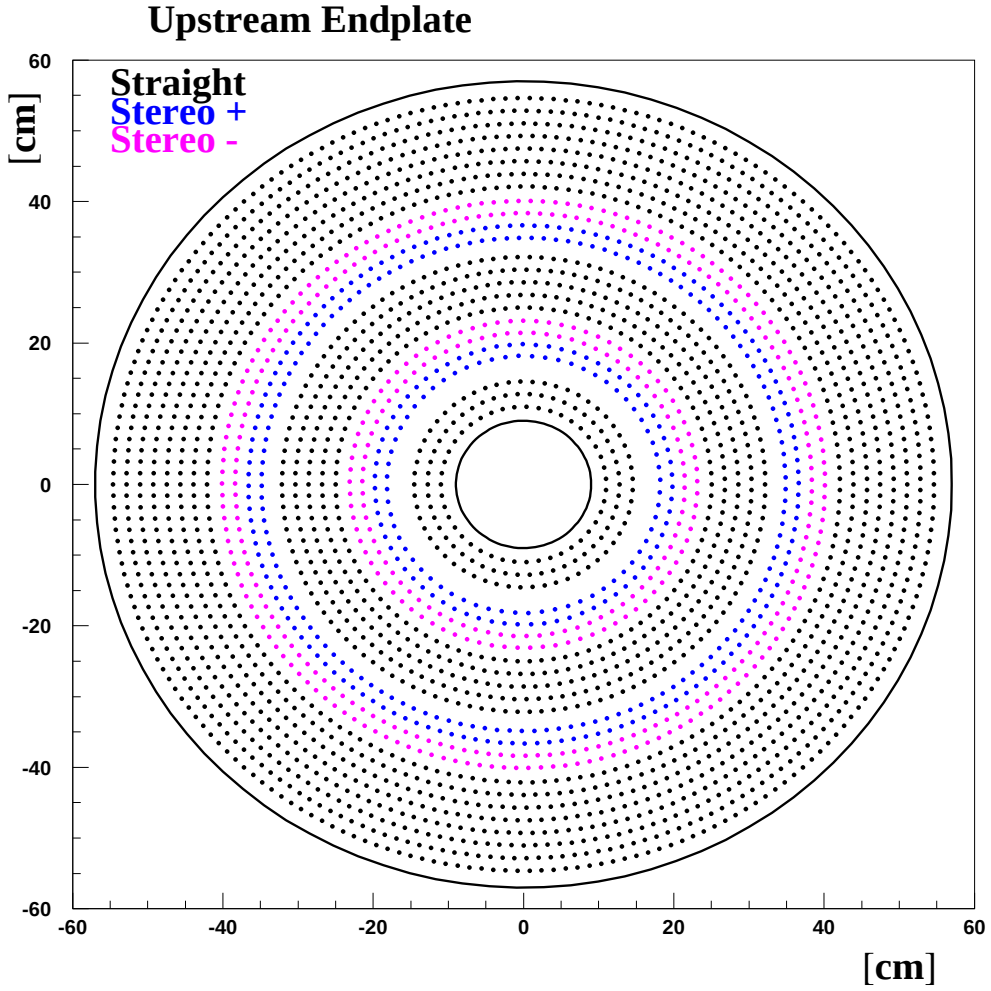

Figure 5: The drill pattern for the upstream endplate using the geometry in table 1. The black dots correspond to straight tubes. The blue dots are the $+6°$ stereo layers, while the magenta dots are the $-6°$ stereo layers.

It is necessary to glue into the donut the insert that both holds the straw tube to the chamber endplate and holds the crimp pin. In order to guarantee a good glue joint between the donut and the insert, a small *glue lip* has been machined on the tip of the insert. If a uniform coat of glue is applied to the outside of the *insert*, then when it is inserted into the donut, the epoxy tends to collect in both the *glue lip* and between the *insert* and the chamber endplate. This is exactly where we need it to be to guarantee a good epoxy seal. Using these specially designed feed-through systems, we are able to obtain a conducting gas-tight joint with all conducting epoxies that we have tried.

These donuts will be machined out of aluminum for the upstream endplate and Delrin for the downstream endplate. These parts have been manufactured at Carnegie Mellon

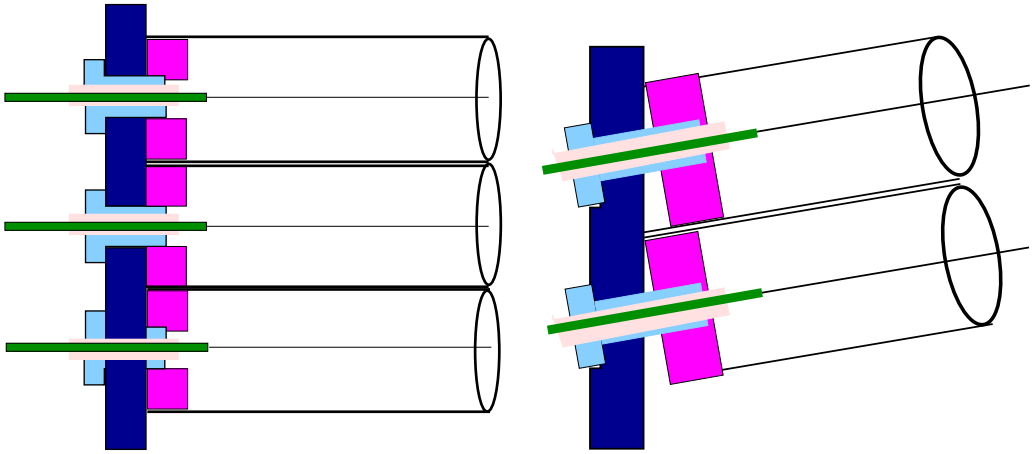

Figure 6: Schematic drawings of the feed throughs for both the normal (**left**) and stereo (**right**) wires in the CDC.

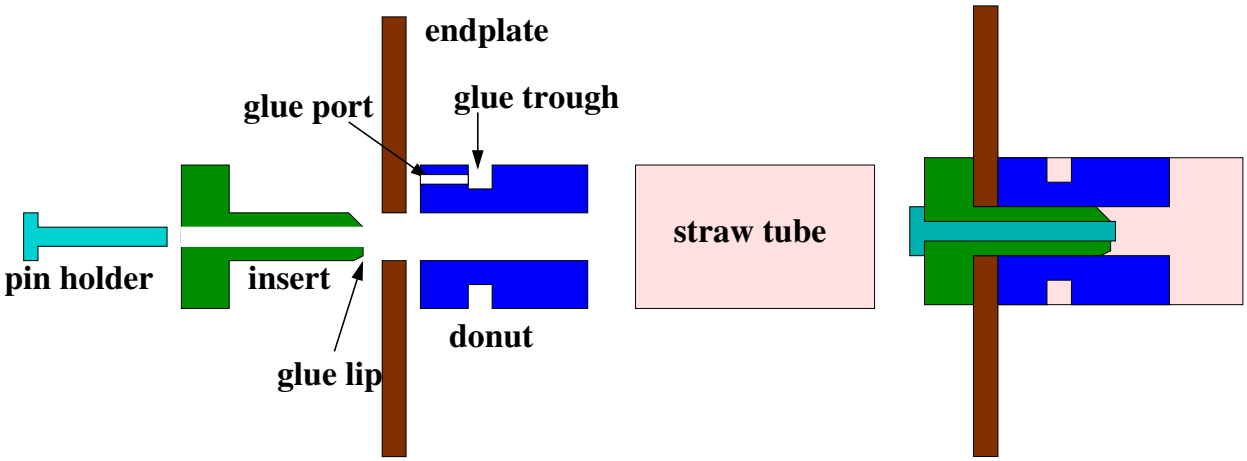

Figure 7: The CMU designed feed throughs that provide a solid glue joint between the straw-tube and the endplate. The left-hand figure shows an expanded view, while the right-hand shows the feed throughs in the chamber endplates.

University for the prototype straw-tube chamber.

Finally, as a backup against leaks in the gas system, we plan to make sure that the shells around the volume containing the strawtubes is also gas tight. This would add an additional layer of safety in case we decide to run some small admixture of a hydrocarbon gas through the chamber. The outer shell is currently planned to by 2mm aluminum shell in two halves, while the inner shell will be $\approx 100\mu$ thick aluminized mylar. Both of these shells can also be used to establish a Faraday cage around the tracking volume.

The straw tubes are clearly a crucial element of the design. Work has been done with both aluminized Mylar and aluminized Kapton tubes. It was found that the Mylar tubes were not particularly forgiving during the construction process. Any kink or bump tended

to remain in the tube, thus destroying its usefulness. In contrast, the Kapton tubes tended to bounce back from just about anything. Once in place, they are much more resilient and significantly less prone to damage. The two main drawbacks to Kapton tubes are the fact that they are somewhat more expensive than Mylar, and that their elasticity makes them more prone to gravitational sag. Gluing them securely to their neighbor tubes in the final chamber is crucial. However, based on experience with both, it has been decided that Kapton tubes will lead to a more resilient chamber, and based on the significantly lower rejection rate (5% versus 95%), will ultimately cost less than Mylar.

2.1 Material in the Downstream Endplate

There are several components to the material in the downstream endplate. The 6mm carbon fiber is the most obvious piece, but the elements which hold the straws in place also contribute. In table 2 are listed the dimensions of these parts. While the the connections

Piece	ID	OD	Length
Donut	0.475cm	0.80 cm	0.70 cm
Insert	0.32 cm	0.475 cm	1.30 cm
Pin Holder	0.26 cm	0.32 cm	1.30 cm

Table 2: The dimensions of the Delrin pieces that hold the straw into the endplate.

of the straws to the endplates do produce local thicker spots (which are accurately modeled in GEANT), it is useful to look at the average thickness of the material in the endplates. Accounting for the holes drilled in the 6mm thick endplate, we have about $1.08\,g/cm^2$ of carbon fiber which represents about 0.025 radiation lengths of material. The Delrin contributes $0.50\,g/cm^2$ to the average thickness, or 0.012 radiation lengths. As an aside, we note that when a 6mm thick endplate was used, it contributed about 0.054 radiation lengths, so at least with respect to the material in the plate itself, this has been cut in half by moving to carbon fiber.

3 The Chamber Gas and the Gas System

The choice of chamber gas plays an important role in the chamber's performance due to the $2.24\,T$ magnetic field. In order to study this, the GARFIELD program [1] has been used to compute electrostatic properties of the straw tubes, both with and without the magnetic field. The results of this study are summarized in a GlueX note [4]. Figure 8 shows an electrostatic calculation for a tube with the wire well-centered in it. Figure 9 shows pairs of GARFIELD calculations, each with a single track going through the straw tube, for three different gas mixtures. The three gas mixtures are Ar(30%)-C_2H_5(20%)-CO_2(50%), Ar(90%)-CO_2(10%), and Ar(50%)-C_2H_5(50%). While in all three cases the time-to-distance relationship is well defined, the longer drift distances of the spiraling tracks introduces a large diffusion contribution to the total resolution. The diffusion resolution, σ_L, is also dependent

on the gas mixture. Pure argon has an extremely poor resolution, while pure carbon dioxide has a very good resolution. Finally, it is desirable to collect the electrons as quickly as possible. A slow gas, or a very long drift distance, can easily increase the collection time over a micro second. For this reason, the Argon-Ethane mixture shown in the lower two plots of Figure 9 is an inappropriate mixture. We expect that an Argon/Carbon dioxide mixture will be appropriate, however, it may be necessary to add a 10% admixture of methane to the mixture. To indicate the advantage of good electrostatics, Figure 10 shows what happens to the time-to-distance relation as one goes from zero magnetic field to full magnetic field.

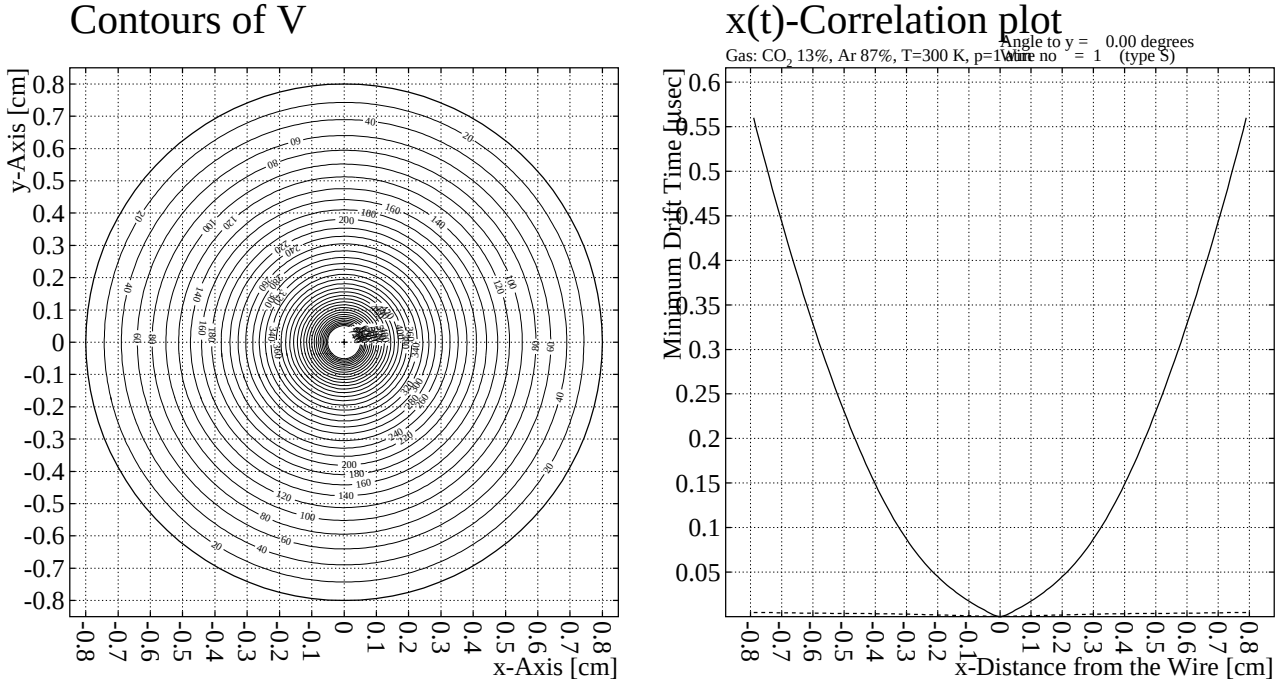

Figure 8: The left-hand plot shows a GARFIELD [1] calculation of the electric field in the straw tube. The right-hand figure shows a typical time-to-distance plot calculated for the straw-tube geometry in the $2.24\,T$ magnetic field.

Currently work is being carried out using a 87/13 argon/carbon dioxide gas mixture. The gas system currently in use for the prototype will likely evolve into the final system. It consists of an MKS electronic mixer that can handle four gas inputs with individually calibrated controls. The resulting mixture is then pushed into a mixing tank, and then delivered to the chamber. The four input gases are filtered before entering the system. One of the gas valves allows for its output to be bubbled through a chilled liquid, such as water or methylal. The current design calls for several gas changes per day in the chamber with the exhaust gas being discarded. Monitors will need to be installed to monitor the temperature and the oxygen content of the input gas. In addition, a slight over-pressure system will be used to keep the gas pressure slightly above the current atmospheric pressure. Such a system will require monitoring the atmospheric pressure and ultimately correcting

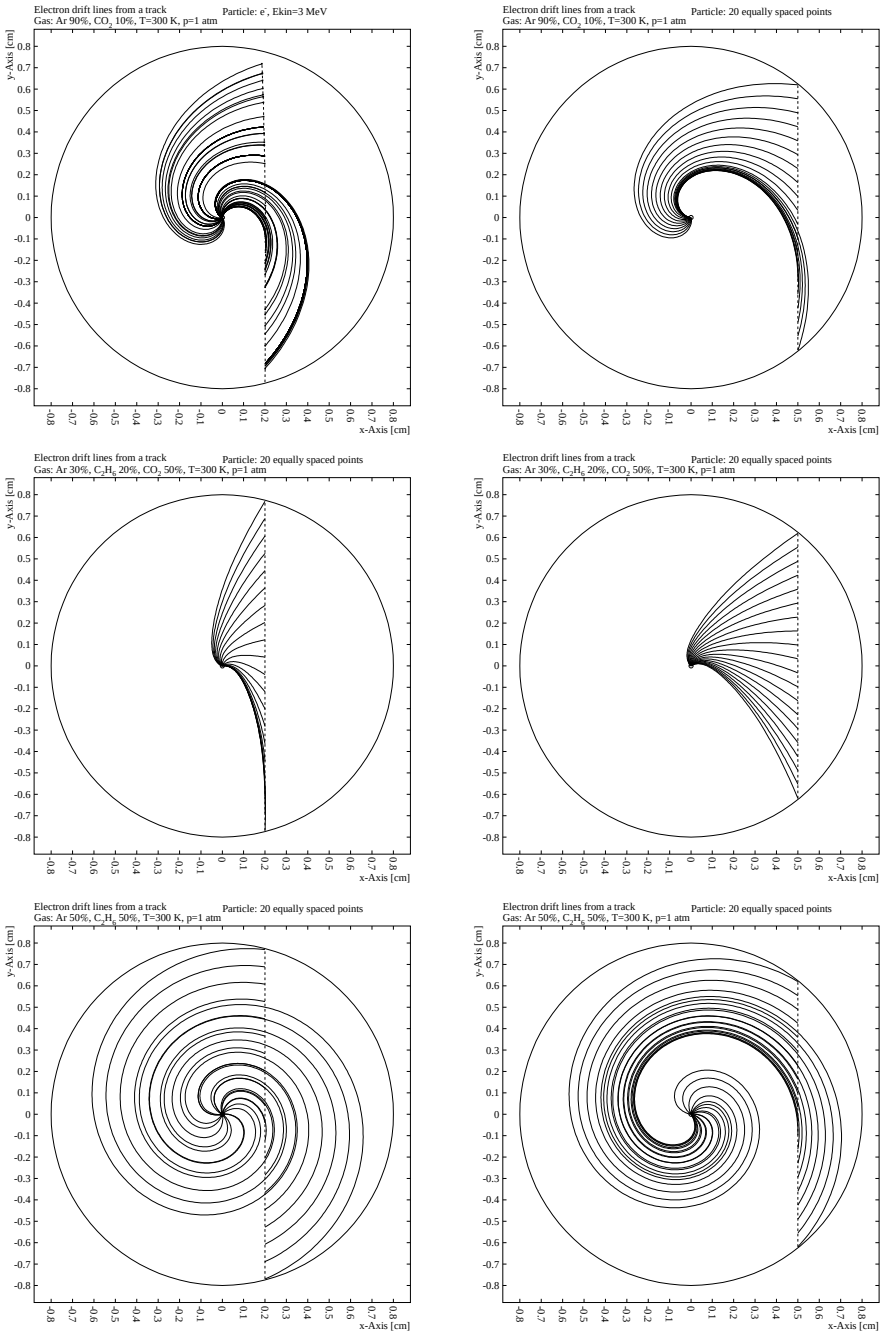

Figure 9: GARFIELD simulations of electrons drifting through a straw tube in the CDC. The curved shape of the tracks is due to the Lorentz angle induced by the $2.25\,T$ magnetic field. The upper pair are for 87/13 $Ar\,CO_2$, the middle pair are for an admixture of a hydrocarbon in the $Ar\,CO_2$ mixture, while the bottom pair are for 50/50 Argon/Ethane. Voltages are different for each to yield similar gas gains.

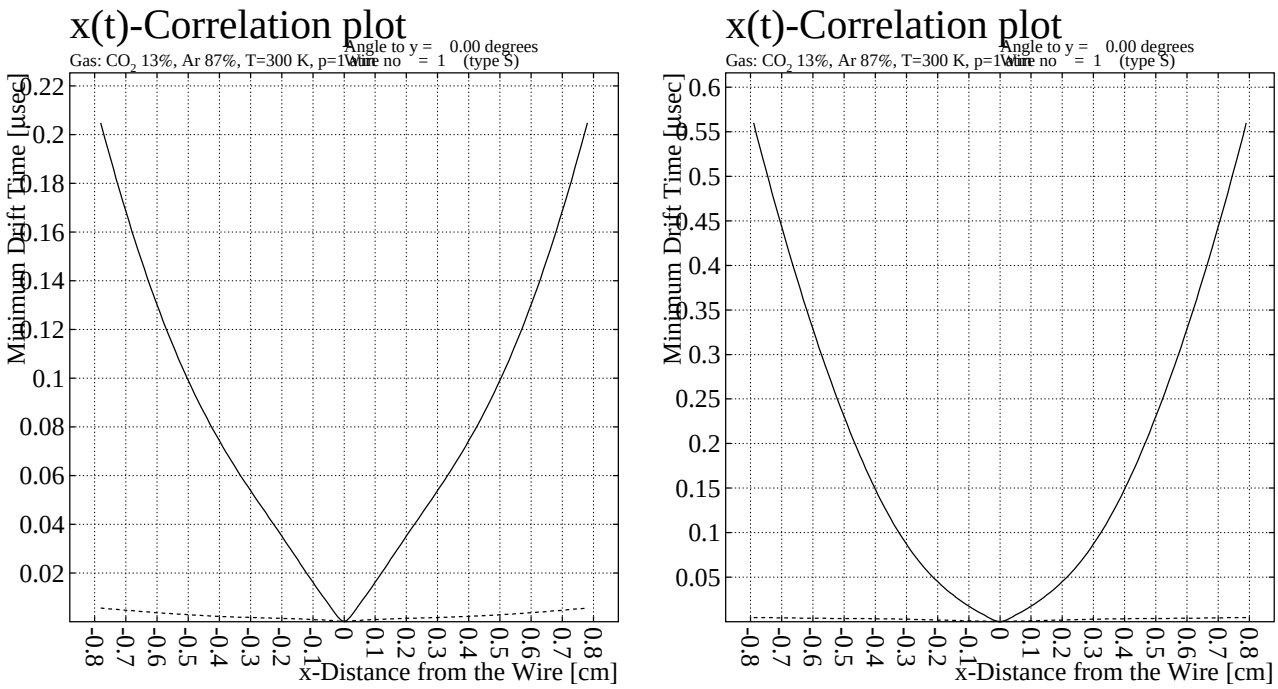

Figure 10: Calculated time versus distance in 87% Argon, 13% Carbon Dioxide mixture. **left**: No magnetic field, **right**: full magnetic field. Both plots are for $1800\,V$ on the anode wire.

the chamber calibrations based on the density of the chamber gas.

The gas system has been designed in consultation with the Environmental Health and Safety group at Carnegie Mellon to allow its use with ethane gas. This work includes a sniffing system that automatically shuts off the flow of ethane in case of a detected ethane concentration near the chamber of a few percent. Using a solenoid-valve, it also automatically shuts off the ethane flow in the case of a power outage.

4 Chamber Position Resolution

In order to achieve the desired $150\,\mu m$ resolution in the CDC, we need to account for all possible contributions to the resolution which are summarized in Table 3. Clearly the most important is the diffusion term, which depends on the gas. A gas mixture that contributes about $120\,\mu m$ for an average $5\,mm$ drift in a $\sim 2.5\,kV/cm$ electric field is required. Many gas mixtures satisfy this requirement. Due to the multi-piece structure for holding the wires in place, we plan to measure the position of the crimp pin at each end of the chamber. This will let us know the position of the center of each pin to an accuracy of $40\,\mu m$. In addition to this, there is a $30\,\mu m$ uncertainty associated in the location of the wire due to the crimping of the wire (a 20μm wire in a $100\mu m$ hole). For a 37g tension on the wire, there is also a calculable gravitational sag that reaches $\approx 41\,\mu m$ at the center of the chamber, and

an electrostatic distortion of about $10\,\mu m$. Both the gravitational sag and the electrostatic deflection scale with the length ($1.50\,m$) squared. The gravitational sag is given as

$$s \;=\; \frac{(\pi r^2)\rho L^2}{8T}$$

where the tension, T, is measured in mass units. The density, ρ, is in g/mm^3, L is the length in mm and r is the radius in mm. Data from wire vendors indicate that the yield point for tungsten wire (where it goes *plastic*) ranges from 65 to 100 grams. In ordering the wire, we will specify as large a yield point as possible, and then string the chamber at a tension of $\frac{1}{2}$ of the yield value. In the case of 65 grams, this would lead to a tension of about 33 grams and a gravitational sag of $54\,\mu m$ which would have little effect on the overall resolution of the chamber. In Table 3 we have used a $41\,\mu m$ sag corresponding to a 37 gram tension on the wire. As is typical in chambers, it is assumed that some reasonable fraction of the gravitational sag can be corrected for.

The timing resolution (how well one measures the drift time using a FlashADC) contributes a position error that is inversely proportional to the slope of the x-t correlation plot shown in Figure 10. It is quite good for large drift times and much poorer for small times. A simple linear approximation to the curve yields a number of about $39\,\mu m$ for times measured to an accuracy of $\frac{1}{3}$ of a time bin (2.67ns). Time fitting algorithms that are matched to the pulse shape in chambers usually yield intrinsic time resolutions around 20% of the time bin width (1.6ns).

The remaining effect is due to diffusion in the gas and goes as the square root of the drift distance. This goes from nothing for zero drift distance, up to about $175\mu m$ for 1cm of drift. All of these effects are summarized in Table 3. Because these the dominant effects depend on drift distance, we have computed plotted our estimate of how the resolution goes as a function of drift distance in Figure 11. We note that the models employed are wrong for very short drift distances where the dominant effect becomes the statistics of ionization along the path length of the track. When all the effects are added in quadrature, we arrive at an overall term that reaches $150\mu m$ over most of the drift volume.

Effect	Resolution μm
Diffusion σ_L	0 to $160\,\mu m$
Geometrical Precision	$40\,\mu m$
Wire Placement in Crimp Pin	$30\,\mu m$
Gravitational Sag	$41\,\mu m$
Electrostatic Deflection	$10\,\mu m$
Timing Resolution	$39\,\mu m$
Design Resolution	$150\,\mu m$

Table 3: The estimated contributions to the ultimate chamber resolution from various known effects. These numbers are based on $1.5\,m$ long, $20\,\mu m$ diameter, Au-W wires under $37\,g$ tension.

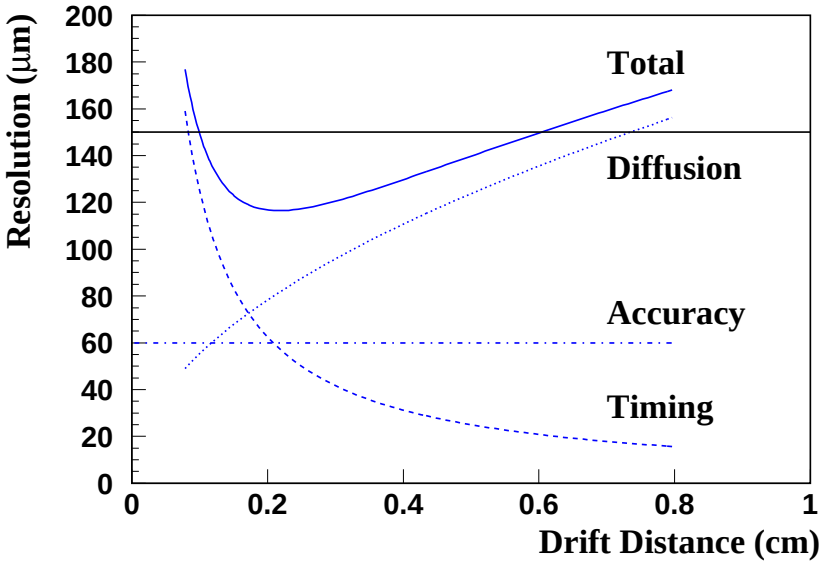

Figure 11: Computed contributions to the position resolution of the CDC.

The position along the length of the wire is measured using 8 layers of stereo wires tilted at $\pm 6^\circ$ relative to the straight layers. The nominal resolution from a stereo layer is given as

$$\sigma_z \;=\; \sigma_{r\phi}/\sin\alpha$$

where $\sigma_{r\phi}$ is the $150\,\mu m$ resolution and α is the stereo angle. For a given crossing, we would get

$$\sigma_z \;\approx\; 1.4\,mm\,.$$

5 Background Rates In The CDC

Electromagnetic interactions of the beam with the target and other material produce the dominant source of backgrounds in the GlueX detector. It is important to understand what these rates are in the CDC. This will limit how close the detector can be to the beam line, as well as the lifetime of the chamber. A detailed study using the Hall-D GEANT (HDGEANT[2]) package has been carried out to calculate the rates in an individual straw tube.

The rates were estimated by effectively counting the number of background particles over the entire length of a straw tube in each of the layers. For a primary tagged photon flux

[2]Currently version 3 of GEANT is used. Plans are to shift to version 4 over the next couple of years.

of $10^7\,\gamma/s$, the measured rates as a function of layer are shown in Figure 12. These can be scaled up by a factor of 10 for $10^8\,\gamma/s$.

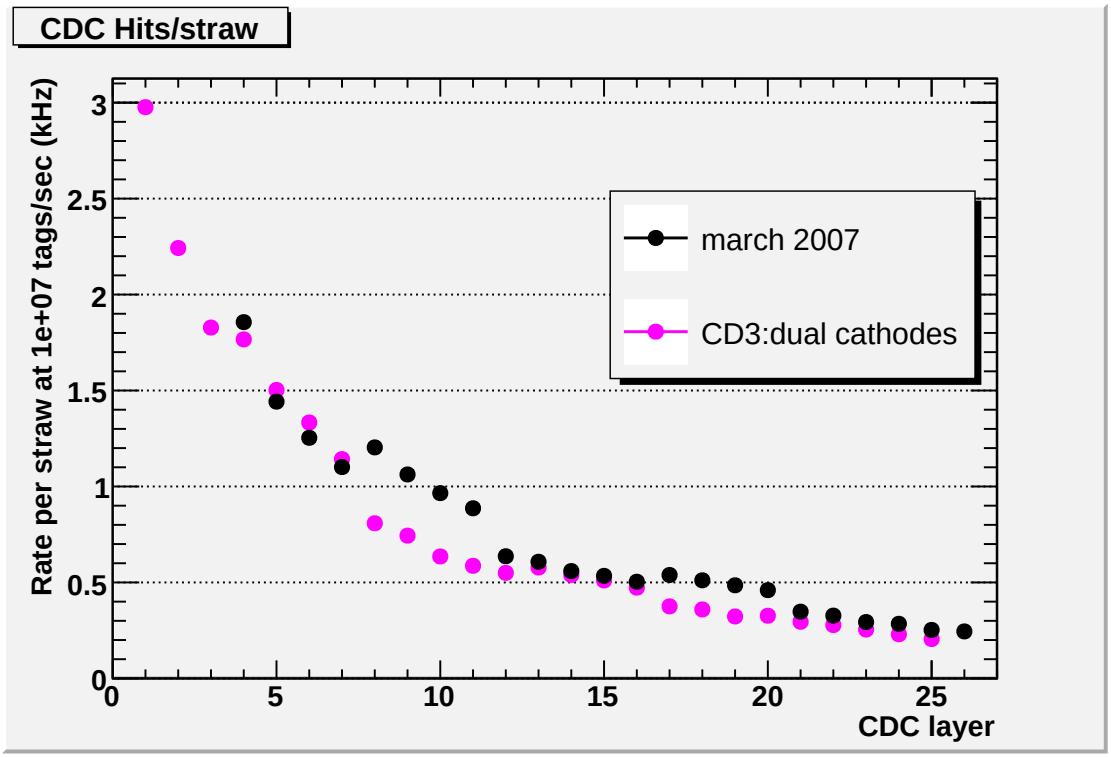

Figure 12: The electromagnetic background rates as a function of layer in the CDC for 10^7 tagged photons per second (the rates are per tube). The relevant plots are the magenta circles. The black circles correspond to a very old design.

The results for the innermost three layers are summarized in Table 4. The highest rates per straw are, as expected, on the innermost layer. At the highest possible rates in GlueX ($10^8\,\gamma/s$), we anticipate a total rate per straw of about $30\,KHz$, a quite manageable rate. Given these numbers, it would appear that it would be possible to move the innermost layer closer to the beam line, perhaps down to about $6\,cm$. However, in such a scenario, the total background rate in the chamber would start to impact the data acquisition system. In addition the material closer to the beam line would degrade the performance of the rest of the GlueX detector. Finally, such a change would also preclude the addition of a future near-target detector which might well be desirable as a future upgrade to GlueX.

Radius	Rate	Channels
$10.9\,cm$	$3.0\,kHz$	43
$12.7\,cm$	$2.7\,kHz$	50
$14.5\,cm$	$1.8\,kHz$	57

Table 4: The computed background rates (for $10^7\,\gamma/s$) for the first three layers of straw tubes in the CDC. Also shown are the number of straws in each layer.

6 Vertex Resolution

The ability to reconstruct the primary, and possible secondary vertexes is an important consideration in GlueX. The CDC is the tracking detector closest to the target, and is therefore the main component involved in vertex reconstruction. Nominally, the closer the measurements are to the beam line, the better the vertex measurement will be. The further one has to project tracks through the magnetic field, the worse things will be. Similarly, for measuring the z-coordinate of the vertex, the radius of the stereo layers in the CDC play a similar role. Simple arguments would advocate moving the first set of stereo layers as close to the beam line as possible to try and match the x-y to the z resolution. Unfortunately, for the stereo layers to provide optimal information, the tracks need to be well mapped (with straight layers) on both the inner and outer sides of the stereo layers. This leads to the configuration in Table 1 where the innermost three layers are straight.

A detailed study of the vertex resolution as a function of where the straight and stereo layers are placed was carried out8 [5]. The results of this study are summarized in Figure 13 where we plot the vertex resolution as a function of the radius of the innermost layer. The layer placement given in Table 1 will lead to a vertex resolution of $\sigma_{xy} \approx 0.5\,mm$ and $\sigma_z \approx 4.5\,mm$. It is also seen that assuming that one could move the stereo layers into $6\,cm$ would only improve σ_z to about $3\,mm$.

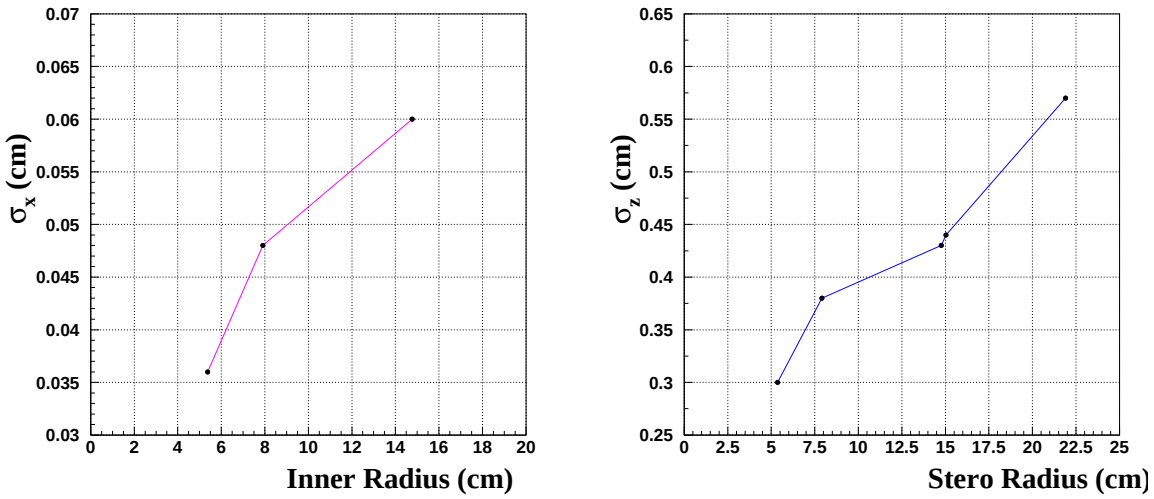

Figure 13: The estimated vertex resolution as a function of the radius of the innermost layer of tubes. (left) For the case of the x resolution, this corresponds to the straight layers. (right) For the z resolution, it is a function of the location of the first stereo layer.

The z-vertex resolution is predominantly driven by the placement of the stereo layers in the CDC and the placement of the stereo layers is driven by two factors: measurement of the polar angle of tracks in the CDC, and measurement of the z vertex position of the event. Both of these criteria require a z measurement close to the innermost radius, however for

the z-measurement to be fully useful, we require straight layers at both smaller and larger radius. This has led us to place the first stereo layer in layer 4 of the CDC. The second set of stereo layers should give a reasonably long lever arm relative to the first, but it is also necessary that the tracks either go through both sets of stereo packages, or if the second package is missed, that at lest the first FDC package is hit. This has led us to place the second set of stereo layers ending at layer 16. Finally, up until the time that the endplates are ordered, it is possible to change the arrangement of stereo and straight wires with no cost or time impact on the construction of the CDC.

7 Chamber Electronics

The on-chamber electronics for the CDC consist of a combination high-voltage distribution and signal translation board and the preamplifier board. It is desirable to have the preamplifier board common between both the CDC and FDC. The high-voltage board is a custom part for the CDC, but most of its individual components will be common with the FDC system. All electronics are designed to have 24 channels, so with 3098 channels, we will need 130 boards to fully instrument the chamber.

The high voltage will be provided by a commercial high-voltage system. Through appropriate segmentation, we will provide positive high voltage to each of the 130 high-voltage boards, and thus to the chamber. We anticipate high-voltage being hooked up in a way that it would be possible to shut off groups of about 5 to 10 preamplifiers at a time in case of a short in the chamber.

A straw tube chamber has the anode wires held at positive high voltage and the surface of the straw tubes held at ground. The ionization electrons, produced by the passage of charged tracks through the tube, drift to the anodes where they undergo gas amplification ($\approx 5 \times 10^4$) and ultimately yield an electronic pulse on the wire. Because both the high voltage and the signal are on the same wire, a special high-voltage distribution board needs to be built that capacitively couples the anodes to the preamplifier. A description of this board is given in reference [6], and the relevant results are summarized here.

The high-voltage board connects high-voltage to the wires in the CDC and couples the signals from those wires to the preamplifier cards. There are several functions that the board performs. First, a low pass filter on the high-voltage input to remove ripples from the line. Second, a current limiter suppresses sudden large currents in the case of a chamber wire breaking and shorting the high-voltage to ground. Finally, a high-pass filter capacitively couple the signal wires to the preamplifier cards. The design specifics of this card are similar to that for the FDC and detailed calculations can be found in the FDC document [7].

The circuitry for the high-voltage board is shown in Figure 14. The high-voltage is supplied at the point HV, and high-frequency noise is grounded out through the low-pass filter of R_1 and C_1, while the resistor R_3 serves as protection in case of a wire breaking. The wire in the CDC is fed through the point labeled Wire. Finally, the signal from the chamber goes through the high-pass filter of C_2 and R_2 and into the preamplifier, which is mounted directly on the high-voltage board. The current design calls for all surface-mount components with $R_1 = R_3 = 1\,M\Omega$, $R_2 = 100\,K\Omega$ and $C_1 = C_2 = 330\,pF$. A justification for these values can be found in references [8] and [7].

The on-chamber electronics mount on the outside of the up-stream gas plenum as shown in Figure 3. The mounting is shown schematically in Figure 15. The design shown here is what is currently employed on the CDC prototype. A pair of custom 12-channel feed throughs allow connection between the CDC and the high-voltage board. In this design, the wires are potted in the feed throughs, soldered to the high-voltage board, then installed on the plenum and connected to the chamber wires. The connection to the chamber is made by putting a small ball of solder on the end of the cable coming through the feed through and then slipping this in a small tube of conducting rubber that slides over the crimp pin on

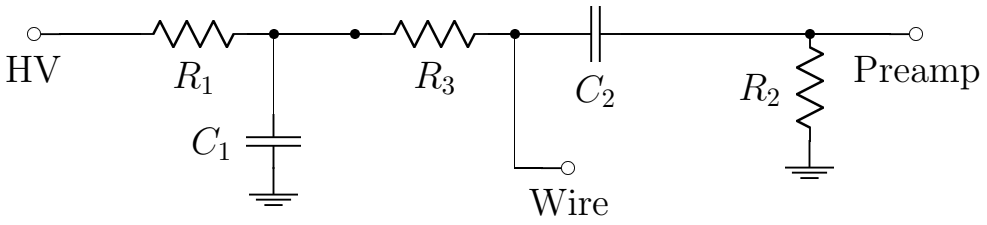

Figure 14: The CDC High-Voltage Distribution Board. In the final design, we anticipate that R_1 and R_3 are $1\,M\Omega$ while R_2 is $100\,k\Omega$. The decoupling capacitor C_2 will be $330\,pF$. The nominal design calls for C_1 and C_2 to be the same to minimize components.

the CDC. This provides a very solid connection to the chamber and is the same procedure that was used in the CLAS region one chamber which was built at Carnegie Mellon about 12 years ago.

We are also investigating a design where a commercial connector is potted into the gas plenum and the high-voltage board plugs into it. While this looks to be a significantly better solution, we are waiting on delivery of the connectors to test this. We note that the final decision on this is cost neutral to the project. We have a solution now that will work and are pursuing improvements to this design that will simplify cabling of the chamber, transportation safety and long-term electronics maintenance.

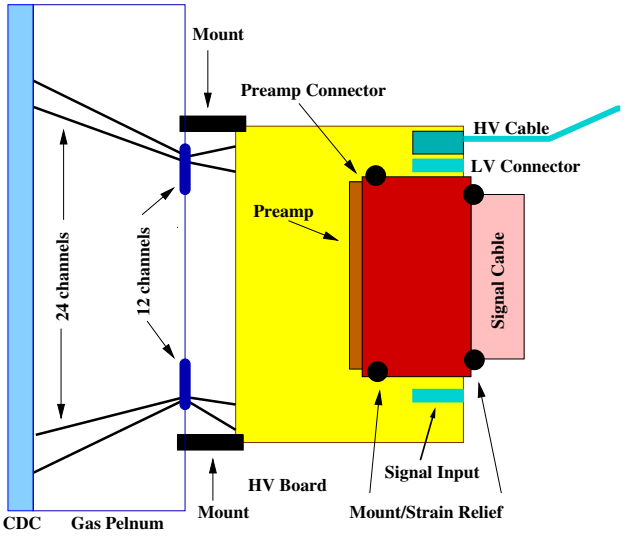

Figure 15: A conceptual drawing of the high-voltage board and preamplifier mounted on the downstream gas plenum and connected to the CDC via a pair of custom feed throughs.

The ASIC preamplifier is being designed by Mitch Newcomer and his group at the University of Pennsylvania in collaboration with Indiana University and Jefferson Lab. The preamplifier card itself has been designed by Jefferson Lab and is currently common with that used by the FDC. The final preamplifier will mount directly on the high-voltage board and then drive a 24-pair cable that will connect into to a shaper electronics designed by

Gerard Visser at Indiana University and in turn, into a custom Flash ADC (FADC) system running at a rate of at least $125\,MHz$. The shaper will be integrated into the input of the 72-channel FlashADC. The same electronic chains will be used for both the CDC and the FDC. Currently, prototypes of all relevant electronics are in use on the prototype CDC. A description can be found in reference [6].

The dE/dx requirement in the CDC requires a reasonable dynamic range in the capability of the ASIC. To separate pions and protons at 350MeV/c requires a factor of 7 in dynamic range, while the path length in going from 90° down to 8° also varies by a factor of 7. However, given the 15ns risetime of the preamplifier, not all the additional charge from the increased length will contribute directly to the pulse height of the low-angle tracks. While detailed studies are being carried out to specify the ASIC, our estimate now is that we need a factor on the order of 100 in dynamic range in the ASIC.

Based on our experience with other chamber systems and what we have learned about straw-tube chambers from other groups, we fully anticipate that grounding is an important issue. There are currently global plans for the grounding of the electronics of the drift chambers as documented in references [9] and [10]. With regard to the chamber itself, the Aluminum on the surface of the straws is connected to the feed throughs using conducting epoxy. The feedthroughs are then connected to the upstream aluminum endplate with conducting epoxy. All components are cleaned before application of the epoxy and all connections are spread over a fairly large surface area to insure a good connection. The endplate of the chamber has a heavy grounding strap that connects to the readout electronics at the level of the high-voltage board. In work with the prototype, we have found that optimal performance is achieved when a solid ground connection between the preamplifier and the chamber is made. In addition, we have found that shielding the up-stream plenum with aluminum foil which is then connected to the heat sink of the preamplifier reduces noise in the system by about a factor of 10. This is discussed in Section 12.

8 CDC Construction

8.1 Chamber Assembly

The assembly of the final CDC is based on experience gained in constructing a 2-meter long prototype at Carnegie Mellon University. For the CDC, most parts will be sent out to commercial vendors. Because of the stereo layers, the endplates will be machined on 5-axis CNC machines. During this process, fiducial marks will be placed on the endplates to allow for later alignment. The feed throughs, crimp pins, wires and straw tubes will also come from commercial vendors. As the parts arrive, they will be visually inspected.

The stringing of the straw-tube chamber occurs in a vertical orientation. The two endplates are placed around an axial tube with support plates for both top and bottom. The tube aligns the two plates radially, but does not fix the angular orientation. This latter step is accomplished with ten support rods which connect near the outer radius of the two endplates. The alignment is achieved by plumbing the two plates relative to each other.

Once the rods are secured to the plates, they remain in place.

After the two endplates have been aligned,straw tube installation takes place. Preparation of the straw tubes starts with a visual inspection to make sure that there are no defects in the straw. Then the straw is cut to the appropriate length (longer for stereo than straight layers). The cutting occurs with a high-speed (10,000 rpm) saw using a very thin blade. The tubes are held in place with a round clamp just next to the point where the cut is made. After the cut is completed, an alcohol covered cotton ball is blown down the length of the tube to remove residual dirt and dust. A picture of the saw is shown in Figure 16.

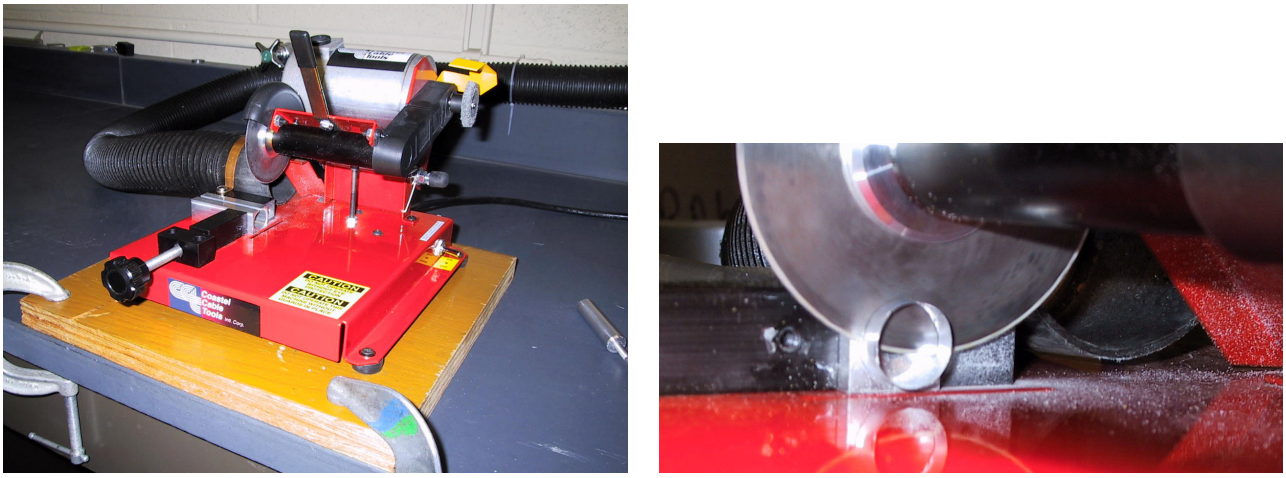

Figure 16: The high-speed saw used to cut the CDC straw tubes to the appropriate length. The black knob on the left-side of the saw tightens a clamp that holds the tubes in place for cutting. The right-hand picture shows a mylar straw being cut by the saw.

At this point, donuts are glued into each end of the straws. These donuts are designed to have a glue o-ring that is filled by forcing glue into the donut with a syringe. It is possible to visibly see when the glue has gone all the way around the tube. These tubes then cure for at least several hours before installation in the chamber. This gluing is shown in Figure 17.

Installation of the straw tubes occurs in a layer-by-layer process. To facilitate this installation, a ring form is machined for each layer that accurately positions the straws at the center of the chamber. All tubes for a particular layer are glued into the endplates using the alignment form, and are then glued, using epoxy, to their neighbor tubes. Also, during installation, the tubes are spot glued to the next innermost layer. Figure 18 shows a photograph of the prototype CDC chamber hung vertically for stringing.

Once all tubes for a particular layer are installed, wires are strung in each layer. The wires are threaded through a magnetic needle that is then lowered through the tube and caught at the bottom of the chamber. The wires are then threaded through the crimp pins. The top is crimped, and then $50\,g$ of tension is applied at the bottom end of the wire, after which it is also crimped. The crimping is accomplished using a pair of pneumatic crimpers whose heads have been machined specifically for the crimp pin. To maintain consistency, the crimp is made by resting the crimping tool on the end of the plastic feed through and then

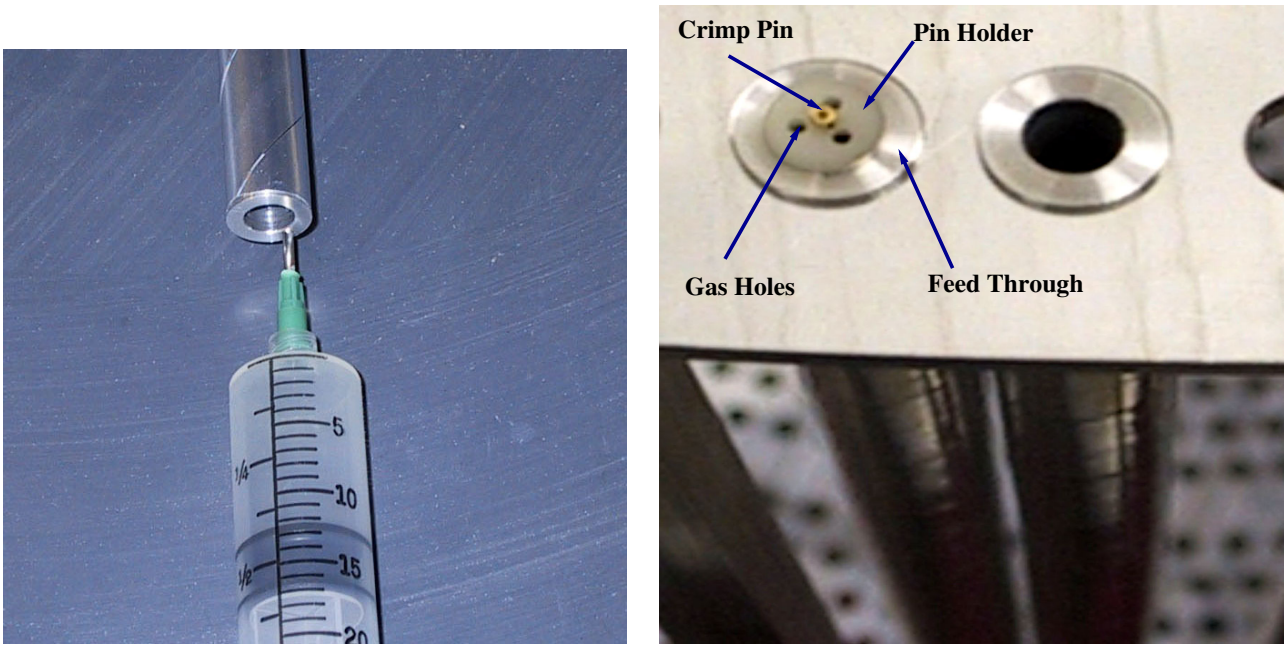

Figure 17: (left) Shows a donut being glued into a straw tube. (right) Shows the feed throughs holding a straw tube in place at the end of the chamber. Note the crimp pin in the center of the pin holder and the three holes to allow gas to flow into the straw tube.

crimping the wire. The crimp occurs a couple of millimeters above the plastic pin holder.

Once a layer is finished, the tension on the wires is checked using a wire tensioning device that works by placing a magnetic field near the wires, then driving the wires with an AC voltage. When the frequency of the AC voltage matches the resonance frequency of the wire, a clear resonance peak is observed. The frequency is then easily converted into actual tension using the wire length and material properties.

The procedure is then repeated for the next layer, moving out until the chamber is strung. For the stereo layers, it is possible to tilt and rotate the stringing apparatus such that the tubes and wires are installed in a vertical orientation. After all wires have been strung, spot checks will be made throughout the chamber to assure that the tension has not slipped. In addition, all wires will be electrically checked to make sure that they have not broken.

At this point, the chamber is brought to a horizontal position and the outside shell is installed. Next the support axis is removed and the inner mylar window is installed. The position of the crimp pins at each end of the chamber will then be mechanically measured relative to fiducial marks on the ends of the chambers. This can be done to a $40\,\mu m$ accuracy and alleviates the need to try and hold extremely tight tolerances on all the feed through components. There will also be an uncertainty of about $30\,\mu m$ associated with crimping a $20\,\mu m$ wire in a $100\,\mu m$ diameter hole.

The downstream gas plenum is then installed, after which the upstream plenum is installed. Independent of which feed through scheme is used, there will be an involved process to connect wires to the crimp pins and bring them through the endplates. To minimize

cabling errors, a detailed spread sheet and check-off list will be used to associate a straw tube with an electrical channel in the readout. After all channels have been wired, a check will be made for shorted wires and bad channels will either be restrung, or disconnected.

At this point, the electronics can be connected to the chamber and high voltage can be applied to all channels. Cosmic rays will be used to verify that all channels are operational. The chamber will then be shipped to Jefferson Lab for installation in the GlueX detector followed by noise studies to optimize the ground connections.

Figure 18: The CDC prototype in its vertical position while straw tubes are installed and wires are strung.

8.2 Construction Schedule For The CDC

Upon completion of the final design for the GlueX CDC, the Carnegie Mellon University (CMU) group will take on the responsibility of building the final chamber for the experiment. This responsibility includes the detector itself as well as the electronics that mount directly on

the detector (high voltage board). The electronics chain from the preamplifiers into the Data Acquisition system will be the responsibility of other members of the GlueX collaboration.

The tasks necessary to build this chamber are shown along with a time line in Figure 19. The start date for this construction project is contingent on funding for the GlueX experiment. The tasks outlined represent approximately three years of work by the CMU group. This plot is reproduced from the overall schedule for GlueX contrsuction.

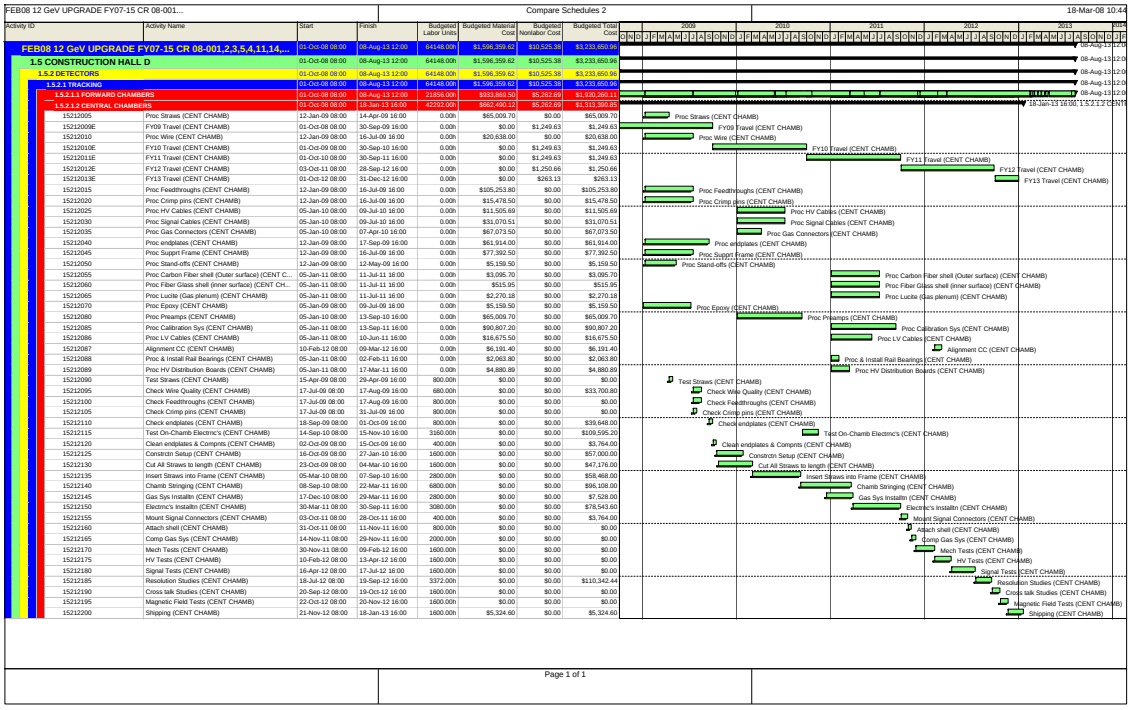

Figure 19: A time line for the construction of the CDC for the GlueX experiment. The overall schedule from start of construction to chamber delevery is a bit over three years.

8.3 Manpower

The Carnegie Mellon University group has primary responsibility for the construction of the CDC. The group in conjunction with the University of Pittsburgh built the Region-I drift chamber for the CLAS detector at Jefferson Lab. In addition, the group has built a number of large planar chambers over the years for use in experiments at Brookhaven National Lab. The CMU Medium Energy Physics Group maintains their own shop in the physics department and employs a full time technician (Gary Wilkin). These resources were crucial in the building of the CDC prototype and will be employed in the construction of the final chamber. Dr. Yves Van Haarlem is effectively full time on the CDC project and we anticipate participation by both graduate and undergraduate students at CMU. We have a long history of involving students in the construction of projects. Finally, Professors Curtis Meyer and Gregg Franklin will both work on the CDC project.

The bulk of the construction effort will come from temporary workers hired to string the chamber. This model was used with the CLAS Region I chamber and worked very well. In the relevant budget documents, we have requested support from Jefferson Lab for a team of three people to work on the stringing of the chamber. One will prepare straw tubes and two will install the tubes and string them.

9 Chamber Installation And Calibration

The CDC will sit on a pair of rails located inside the solenoidal magnet (see Figure 20). For installation and extraction of the chamber, the rails will *mate* with external rails mounted to a cart on the upstream side of the detector. The CDC will be able to be inserted and extracted with its cabling intact. Positioning of the chamber will include fiducial marks that can be surveyed, as well as all possible positioning pins. The positioning system still needs to be designed. It is crucial that the relative position of the CDC and the FDC be accurately known in order to achieve the ultimate required resolution. In addition, for regions where the magnetic field is not uniform, it will be necessary to know the absolute locations of the chambers relative to the magnetic field with reasonable accuracy.

For electronic calibration of the chambers, there will be a system that sends pulses to the inputs of the preamplifier. This will allow for a relative timing measurement of each channel as well as a method to monitor gain variation in individual channels. As noted earlier, it will also be necessary to monitor the gas pressure and temperature and then make corrections for density changes in the gas.

A geometrical alignment with the FDC is anticipated using data with the solenoidal field turned off and alignment of straight tracks between the two chamber systems.

The starting point of the reconstruction will be a time-to-radius relation that can be accurately calculated using the GARFIELD program. With this as a starting point, we anticipate being able to select a reasonably profuse reaction that can be reconstructed and then used to fine tune the calibrations.

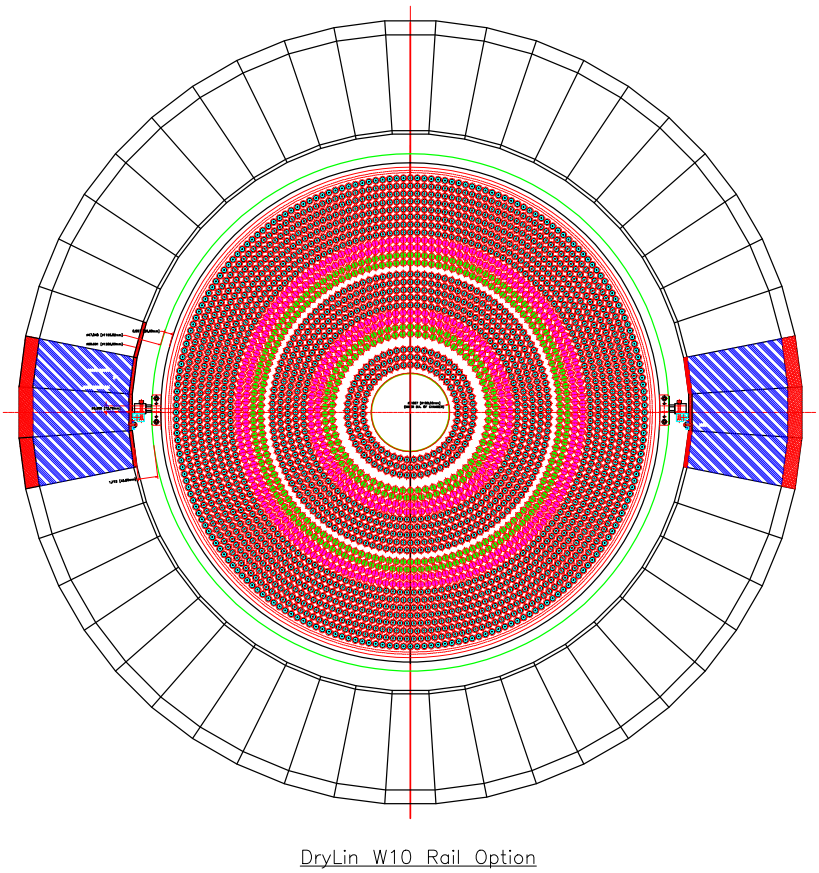

Figure 20: The CDC sitting on support rails in the final GlueX detector.

10 Chamber Maintenance

The CDC is designed such that all of the electronics are on the upstream end of the chamber. These will be accessible without removing the chamber from the magnet. In the case where a wire were to break and short out against the side of the straw tube, we anticipate that the high voltage will be distributed in blocks such that some section of the chamber could be turned off. It is also possible from the upstream end to disconnect a high voltage channel on the board for a single wire. However, the operation of moving things out of the way may well make this a one to two shift long operation.

11 Safety Considerations

The CMU group has an excellent working relationship with the CMU Environmental Health and Safety (EH& S) Department. Input from EH& S is sought on all issues that could impact safety at Carnegie Mellon University. During the many years that the group has built major pieces of equipment, there have been no injuries.

The installation procedure for the CDC, including all needed rigging, will be worked out in conjunction the the Hall engineer and the Jefferson Lab safety group. The chamber is not overly heavy, but it will need to be handled carefully and safety procedures for both personnel and hardware will be developed.

During chamber operation, the most likely safety concern is the chamber gas. At the moment, the gas mixture contains only argon and carbon dioxide and is not considered dangerous. There is some chance that the ultimate gas mixture will contain a small ($\approx 10\%$) admixture of a hydrocarbon (methane). We note that in the gas system we built for the prototype, it is possible to mix ethane into the system. In conjunction with the CMU EH& S group, we designed the system to incorporate a gas sniffer that would shut of the ethane if a few % concentration of ethane were detected leaking from the system. We anticipate a similar system for the final chamber where we would measure the concentration in the gas mixture and take appropriate automatic action if problems occur.

Another area of concern with the chamber is the high- and low-voltage systems. These are all commercial units which are being specified by the JLab group and will meet all JLab safety requirements. These units will allow for appropriate current limits to be placed on the chamber components.

We also have some concerns about eddy currents resulting from a magnet quench. The outer shell of the CDC will be broken into several isolated pieces around the circumference of the chamber. Effects on the upstream endplate are still under study.

12 The Full-scale Prototype

Over the last several years, the Carnegie Mellon group has performed a significant amount of R&D work related to the CDC. This work included the construction of a $2\,m$ long chamber that represents $\frac{1}{4}$ of the circular endplate. As a historical note, the $2\,m$ length was the original proposal for the length of the CDC, which has since, through a series of studies been reduced to the currently planned $1.5\,m$ length. The prototype contains about 70 straw tubes, of which most have been strung with wires. The straws included both aluminized mylar and aluminized Kapton. In addition, straight and both directions of stereo layers have been installed, with particular emphasis paid to the transition from one to another. Figures 21 and 22 show pictures of the prototype on the test bench at CMU.

Various material questions were addressed through the prototyping period, most of which have been summarized earlier in this report. Initially, we determined that the endplates would need to be produced as single pieces, which will require an external firm to take on the job. Test with two-piece endplates (octant) showed that we could not maintain relative

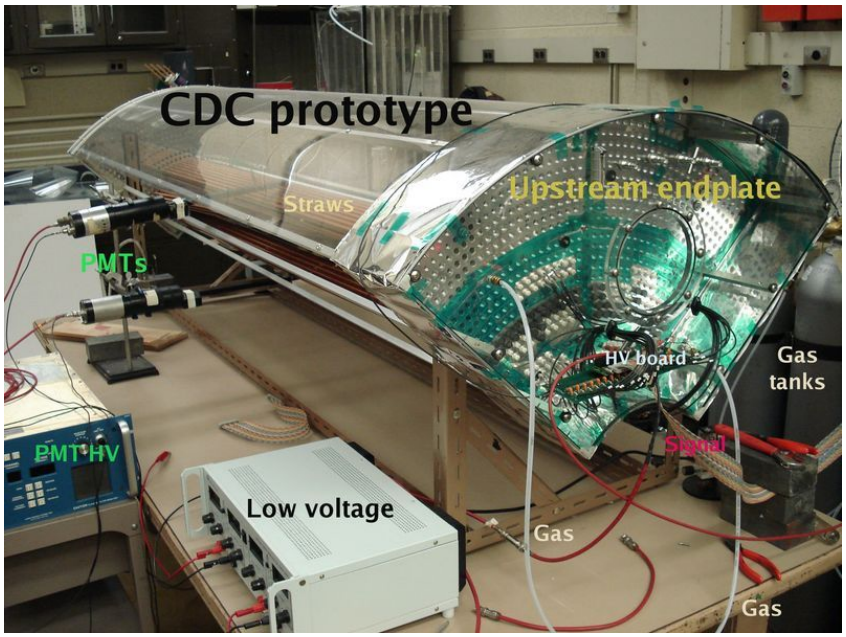

Figure 21: A photograph of the $2\,m$ long CDC prototype at Carnegie Mellon. The copper-colored tubes are Kapton and the silver-colored ones are mylar. Also shown are a pair of small scintilla tors used in a specialized cosmic trigger.

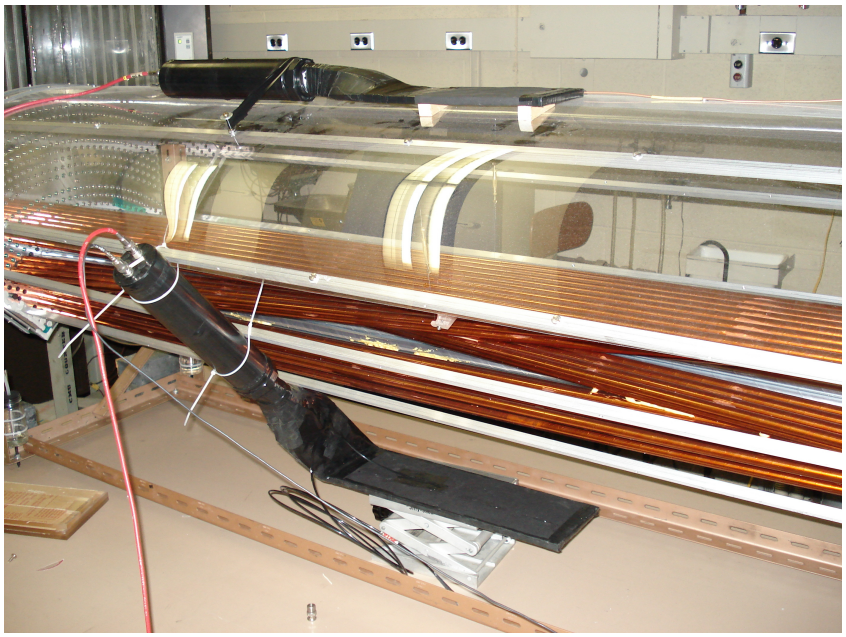

Figure 22: A photograph of the $2\,m$ long CDC prototype at Carnegie Mellon. The copper-colored tubes are Kapton and the silver-colored ones are mylar. Also shown are a pair of scintillators used in a specialized cosmic trigger.

position accuracy at the desired level. Tests were also made with both Mylar and Kapton tubes, with a final decision made in favor of Kapton. This is driven by both robustness and cost. We have also manufactured samples of all of the parts that will be used in the final chamber. This includes feed throughs, gas plenums, electrical connections, and high-voltage board.

The prototype chamber currently has sixteen instrumented channels (the number of flash-ADC channels available), and is set up to collect cosmic ray events using a pair of roughly $20\,cm$ by $20\,cm$ scintillators placed above and below the chamber with about $80\,cm$ between them. The signals from the chamber go through a second generation high-voltage board that contains the capacitors that will be used in the final board. This board has 16 rather that the final 24 channels that will be used. A prototype ASIC preamplifier is plugged into the high-voltage board. This preamplifier board has two of the three eight-channel ASIC chips on it. We note that a final run is planned on the ASIC later in 2008 based on feed-back from both the CDC and FDC studies. The preamplifier board outputs a differential signal that goes through a $18\,m$ long, 24-channel twisted-pair cable. The cable, in turn, plugs into a 16-channel receiver/shaper board[3]. The output from the shaper board then goes to two 8-channel, $200\,MHz$ commercial Flash ADC board (Struck Sis3320) in a VME 64x crate. The Flash ADC's are then read out using CODA 2.5, the Jefferson Lab data acquisition system that will be used in GlueX[4]. In table 5 are summarized what is used in the prototype and what is planned in the final chamber. In nearly all cases, we are using something very close to what is planned in the final chamber.

12.1 Noise Reduction

Minimizing noise pickup in the CDC is important to enable the best possible resolution in the final chamber. In this section we detail some of the work that has been done with the prototype and point out the important lessons that will be crucial in the final chamber construction. Most of these steps involve shielding and grounding of the chamber and the electronics. We highlight this work by three pairs of plots, each of which shows a *before* on the left and an *after* on the right. The first (Figure 23) shows pulses seen on the prototype. The before plot on the left shows fairly significant noise everywhere along the pulse and also a significant *ringing* just before the physics pulse. This ringing was thought to be associated with a computer monitor about two meters from the electronics. The right-hand pulse shows the substantial noise reduction achieved. On the scale shown, it is almost impossible to see the noise on the chamber.

An alternative way to look at this is to look only at the pedestal signal on a straw. Figure 24 shows a pair of scope traces for the same channel for both before and after. Both traces are on the same scale (on the scope) of $2\,mV$ per division. The noise is well under a mV after improvements. Finally, Figure 25 shows a plot of the data in the pedestal bins

[3]The version to be used in the final chamber will be integrated into the 72 channel, 125MHz FlashADCs.

[4]CODA is actually evolving towards version 3, and at some point in the future the local system will be upgraded to the newest version of CODA.

Element	Prototype Chamber	Final Chamber
Straw Diameter	1.6 cm	1.6cm
Straw Length	2m	1.5m
Wire	20 μm	20 μm
Voltage	+1800 V	+1800 V
Gas Mixture	87/13 $ArCO_2$	87/13 $ArCO_2$ (possible small hydrocarbon content)
Magnetic Field	none	2.25T along wire length
HV Board	Final Components, v3	Final Components, v4 (smaller board, imported ground connects)
Preamplifier	Prototype ASIC	Final ASIC
Cable	Final Cable, 18m	Final Cable, 14m
Shaper	Prototype Version	Final Version (stretched pulses and impedance matched)
Flash ADC	200MHz commercial	125MHz custom
Readout	CODA v2.5	CODA (version under development)

Table 5: A comparison between the prototype and the final CDC.

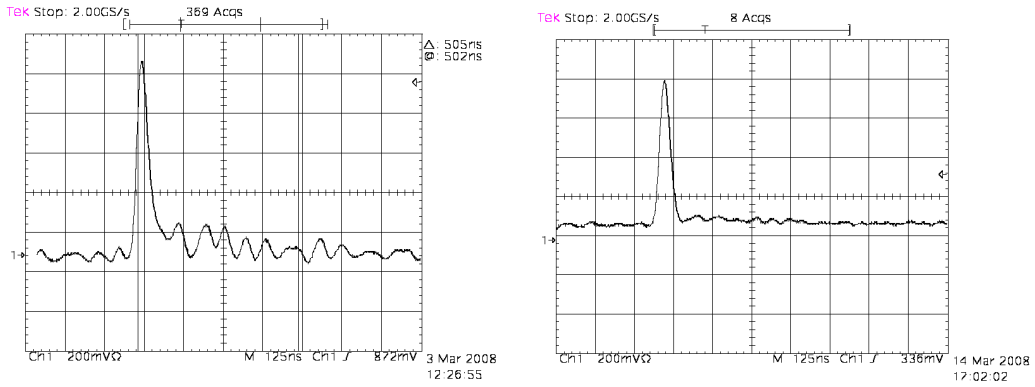

Figure 23: (left) A signal pulse as seen on a straw before work on grounding and noise reduction. (right) A signal pulse after improvements. Both plots are on a 200 mV per division scale. Note the noise at nearly 100 mV peak-to-peak before reduction. After reduction, the noise is essentially invisible on the trace. These signals are observed after the shaping electronics.

from the FADC system for both before and after. The point to note here is the relative widths of the two distributions. The before plot goes from roughly 300 up to 1500 channels, while the after goes from roughly 860 to 1060. The absolute value is not relevant, but the reduction in width is very significant.

There have been a number of attempts to reduce noise. These included heavy grounding straps for the chamber endplate to various points in the electronics, wrapping the straw tube volume with grounded foil, wrapping the gas plenums with foil, and multiple and

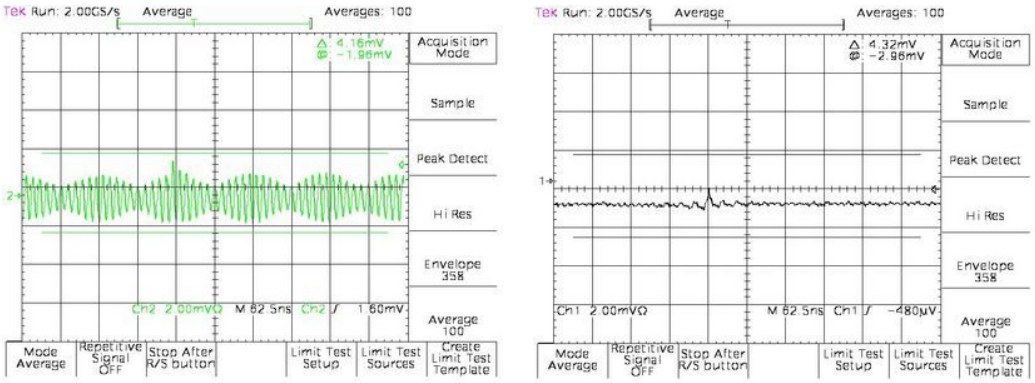

Figure 24: (left) Noise on a straw before work on grounding the prototype. (right) The noise on the same channel after the grounding. The noise has been reduced by about a factor of 10. Both plots are on $2\,mV$ and $62.5\,ns$ per division scales. These signals are taken at the output of the preamplifier (before the shaper).

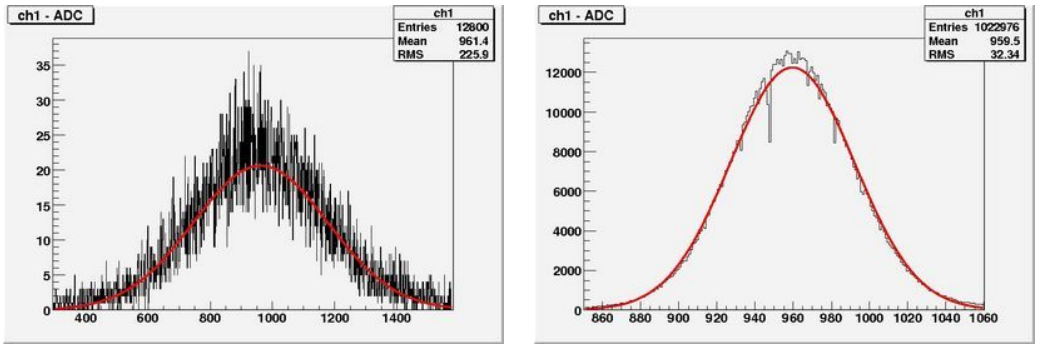

Figure 25: (left) The pedestal on a straw before work on grounding and noise reduction. (right) The pedestal on the same channel after improvements. Note that the final pedestal is significantly narrower than what it was originally.

varied combinations of the above. The most significant reduction (nearly all the factor of 10 that was achieved) was accomplished by wrapping the upstream gas plenums in grounded foil and making a single solid ground connection from the endplate to the high-voltage board, and connecting the heat strap on the preamplifier board to the foil around the up-stream gas plenum.

Based on this work, we believe that a heftier ground connection between the preamplifier board and the high-voltage board is needed. This then needs to be grounded to the endplate of the chamber. It also appears quite important to have the up-stream gas plenums wrapped in shielding foil.

While we recognize that the final chamber as installed in the GlueX detector will have its own grounding issues, the lessons learned with the prototype have shown us what to look for in a grounding plan for the electronics in final chamber. We note that the design of the final chamber includes an aluminum shell around the straw volume and shielding of the gas

plenums. The electronics will also include thicker ground connections between parts and the possibility to add additional grounding connections between the endplate and electronics.

12.2 Pulse And Track Fitting

There are several methods to fit drift time using Flash ADC data. The most common is the so-called first electron method which we will be describe in some detail. Alternatives include the differential center of gravity and fitting pulse shapes to the rising edge of the pulse [11]. All of these methods start by subtracting the pedestal from the measured signal. The pedestal is generally measured, either on a pulse-by-pulse basis, or by taking special triggers on a regular basis to track it. The first electron method fits a straight line to some part of the rising edge of the pedestal-subtracted pulse, and then takes the intercept of the line with the amplitude axis (pulse height) to be the drift time, (arrival time of the first electron). For the following, we will assume that we have pedestal-subtracted data.

In fitting to the leading edge, there may be some choice in what part of the data to use. We show a pedestal subtracted pulse in Figure 26. There are four points on the leading edge, but a choice for fitting could be the first n, where $n = 2, 3, 4$, or we could ignore the first point and then fit the 2'nd and 3'rd, or the second, third and fourth. Typically, one would like to ignore the first point, but it is also desirable to have more than two point to fit to. In such a scenario, one would like the leading edge of the pulse to be roughly four to five FADC channels long, which usually implies that the pulse is shaped to achieve this.

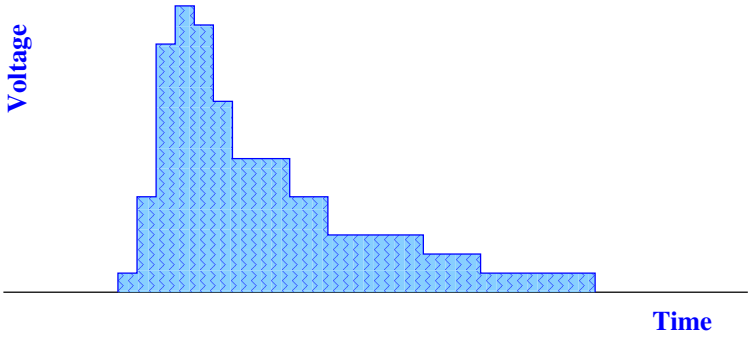

Figure 26: A schematic of a pulse as seen in the flash ADC system. The rising edge covers four time bins, while the fall-off is quite a bit longer.

In the following, we assume that we will fit the first n points of the pulse. Along the rising edge, we have several pairs of points, (y_i, t_i). These are fit to a straight line to yield a slope α and intercept y_0.

$$y \;=\; y_0 + \alpha t$$

Doing a simple least squares fit, we can solve for y_0 and α by computing a number of sums. If there are n points along the leading edge used in the fit, we find that

$$y_0 \;=\; \frac{\sum_{i=1}^{n} y_i \sum_{i=1}^{n} t_i^2 - \sum_{i=1}^{n} t_i \sum_{i=1}^{n} y_i t_i}{n \sum_{i=1}^{n} t_i^2 - (\sum_{i=1}^{n} t_i)^2}$$

$$\alpha \;=\; \frac{n\sum_{i=1}^{n} y_i t_i - \sum_{i=1}^{n} t_i \sum_{i=1}^{n} y_i}{n\sum_{i=1}^{n} t_i^2 - (\sum_{i=1}^{n} t_i)^2}\,.$$

From these, the first-electron drift-time of the pulse is defined to be the intersection of the line with the $y = 0$ axis and can be computed from y_0 and α as follows,

$$t_e \;=\; -\frac{y_0}{\alpha}\,.$$

For the pulse shown in Figure 26, we report the computed t_0 based on the first 2, 3 and 4 bins of the rising edge. The reported t_0 is the fractional bin width as measured from the edge of the first bin. Over varying pulse shapes and sizes, one typically finds an uncertainty on the order of $\frac{1}{4}$ of a bin width with 3 to 4 samples on the rising edge. Table 6 shows these fits for the given pulse.

n	y_0 (amplitude)	α (amplitude/time)	t_e (fractional time bin width)
2	-0.75	5.0	0.15
3	-0.78	6.0	0.13
4	-0.26	4.9	0.05

Table 6: Fit first-electron times from the pulse shown in Figure 26.

Data from a large number of pulses are collected and the measured drift time for each channel is looked at. A fit is made to determine what the earliest time on each channel j is, t_0^j. In analyzing data, the drift time utilizes both the t_0 and the first electron time, t_e to yield the drift time.

$$t_d^j \;=\; t_e^j - t_j^0$$

Using the resulting t_d^j, a look-up table computed using GARFIELD (see section 3) converts the drift time to a distance from the wire, r^j. This distance is then combined with the location of the wire (x_w^j, y_w^j) to define a *drift circle* to which the primary track is tangent. Figure 27 shows an example of a track going through four straw-tubes. The drift circles are shown around each of the four wires. A fit can be done to then define the best track parameters that reconstructs tangent to all the drift circles. An examination of Figure 27 indicates that there is no other track candidate that would fit as well as the true track shown in the figure.

In fitting pulses, good timing resolution is obtained when one has 3 to 5 samples on the rising edge of the pulse. Figure 28 shows a histogram of how many samples are observed in the prototype using 200MHz FlashADCs. The average of this is a bit more than 6 samples, which corresponds to a 30ns risetime of the pulses in the CDC. In the final chamber, we currently plan to use 125MHz FlashADCs. This causes the sample time to increase from 5ns to $8ns$, and subsequently requires us to configure the shaping electronics to stretch the rising edge of the pulse from about 30ns to about 55ns.

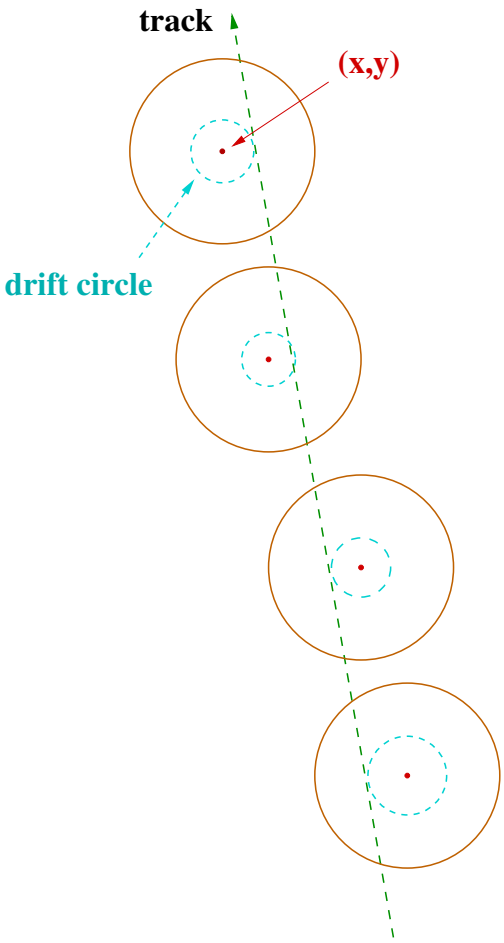

Figure 27: A track going through four straw tubes in the CDC. The straw tubes are shown as the large circles and the location of the wire is indicated as the dot at the center of the circles. The track passes through the wires and the first ionization in each tube comes from the point where the track intersects the dashed circle inside the straw tube. Fore each hit, we then have the (x, y) coordinate of the wire and the radius of the dashed circle.

12.3 Chamber Resolution Studies

Resolution studies in the CDC prototype have been performed. Sixteen channels which span six layers in the CDC have been instrumented and are read out using the electronics described above. Cosmic events are triggered using a pair of $20\,cm$ by $20\,cm$ scintillators placed above and below the chamber. The chamber is run using a 87/13 mixture of $Ar\,CO_2$ gas with a nominal voltage of $1800\,V$ on the anode wires. Data runs go for roughly 24-48 hours after which sufficient statistics have been collected to look at chamber resolution.

As the trigger may change from run to run, the first step in the analysis is to determine the t_0 (see Section 12.2) for each wire. The data are then analyzed to get the drift time from each found pulse. Events with more than three straws hit can then be used for resolution

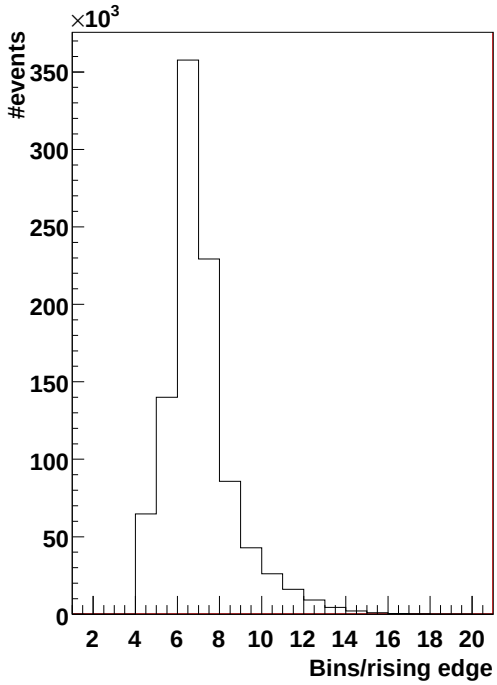

Figure 28: A histogram of the number of samples on the rising edge of the pulse as seen in the CDC prototype.

studies. The most optimal events for these studies involve events which have hits in each of the six instrumented layers, but given the low rate of cosmics, and the relatively large size of the paddles, these are not particularly common.

Before starting, we need to make an estimate of what we should expect for the resolution in zero magnetic field using a 200MHz FlashADC. To do so, we follow the discussion in section 12.3. From the data in table 3, we expect that the timing resolution will change. As an approximation we treat the time-to-distance relation for zero field as a linear approximation with a drift speed of $v_d = 8000\mu m/220ns$. This then leads to a error in position due to timing of $\Delta x = (36\mu m/ns)\Delta t$. With a 200MHz FlashADC, the time bin is 5ns, and taking $\frac{1}{4}$ of this, we have $\Delta t = 1.25ns$. This leads to a roughly flat contribution of about 45μm. If we compute the expected resolution function, we find the plot as shown in Figure 30. Here we expect to observe resolutions that are smaller than the anticipated 150μm.

To determine the resolution, tracks are found and fit as described in the previous section. One measure is to fit the line and then look at the residual for each hit to the fit line, r_j. This residual is smaller than the resolution, and the factor varies based on the geometry of the chamber. However, there is a simple formula [12] which allows us to calculate a scale factor, g_j, for each residual. The resolution of each anode is then given as

$$\sigma_j \quad = \quad g_j r_j \, .$$

We have n possible measurements along a track, with the position of the j^{th} anode given as x_j. We also define a factor a_j for each anode that is 1 when the anode is used in a track and

Figure 29: A scale drawing showing the relative orientation of the straws used in the resolution studies.

0 when it is not. From this, we compute the averages of the anode position,

$$< x > = \sum_{j=1}^{n} a_j x_j$$
$$< x^2 > = \sum_{j=1}^{n} a_j x_j^2$$

and from this define the quantity N to be

$$N = < x^2 > - < x >^2$$

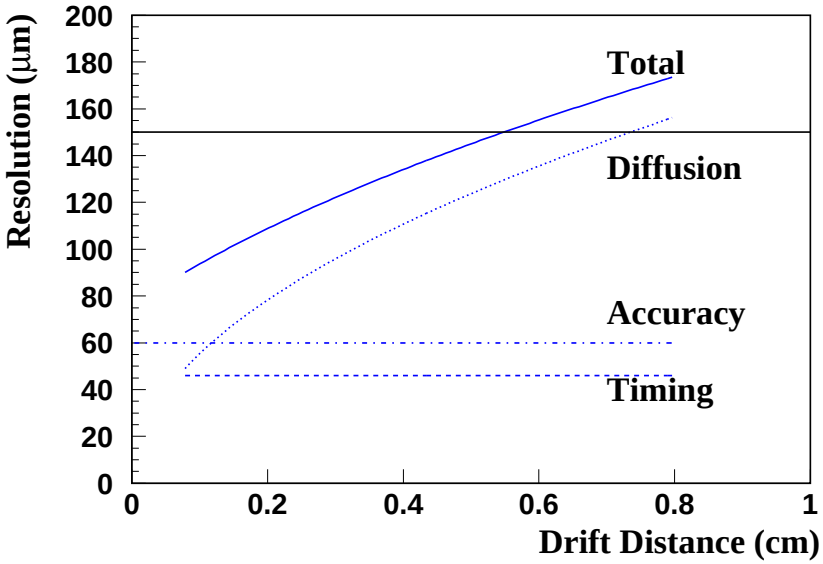

Figure 30: The estimated contributions to the prototype resolution in zero magnetic field.

For a fit including m of the n anodes, we define a g_j factor for each of the hits anodes as

$$g_j \;=\; N\left\{\sum_{k=1}^{n}\left[a_k\left(< x^2 > - < x > (x_k + x_j) + m x_k x_j\right) - \delta_{jk}N\right]^2\right\}^{-\frac{1}{2}} .$$

The computed resolutions for three of the wires are shown in Figure 31. The distributions are typically a Gaussian with a tail. At present, we do not fully understand the tail, but it is likely due to adding noise hits to the tracks. The resolutions determined from fitting lines to the tracks vary from about $80\mu m$ up to $142\mu m$. Those shown in Figure 31 are 127μm, $111\mu m$ and $123\mu m$.

12.4 dE/dx Studies In The CDC

Studies of performing dE/dx in the CDC have just started using cosmic tracks. The JETSET detector at LEAR showed that it is possible to do dE/dx measurements in a straw tube chamber [3]. Our work will follow somewhat what they did. The crucial detail that makes dE/dx in a straw different from a more conventional drift chamber is the fact that the path length of a track inside a given straw can very by large factors. This comes about both from how close to the wire the track crosses, but also the angle relative to the wire length at which the track crosses. Figure 32 shows schematically two tracks crossing through a straw tube with quite different lengths in the straw.

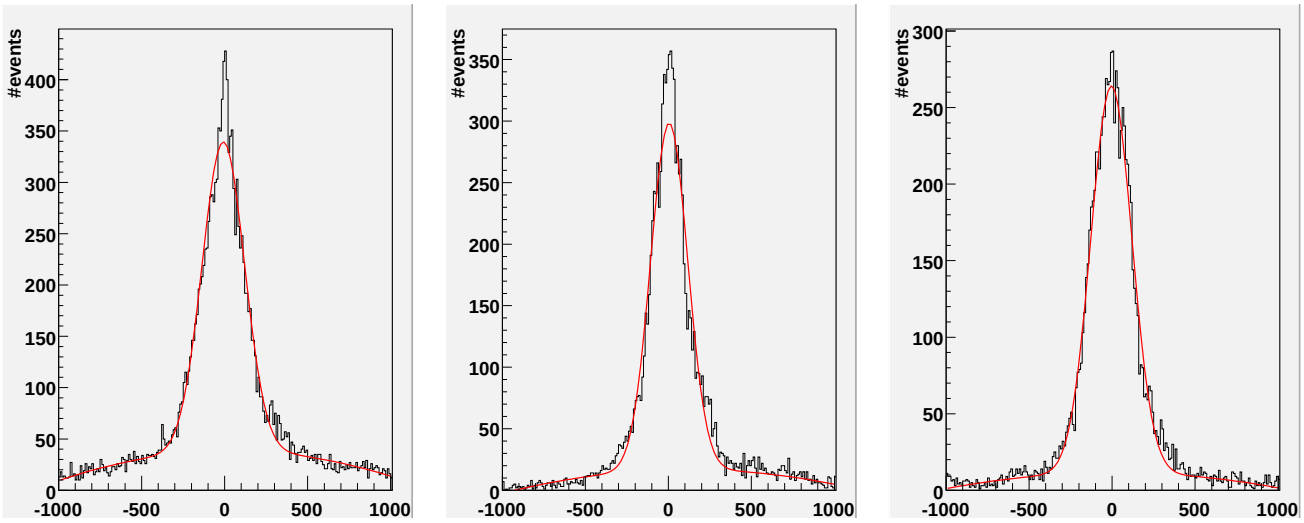

Figure 31: Measured resolution in the CDC prototype on three wires. The units on the horizontal axis are μm. The Gaussian fits scaled by the g factors yields 127μm, 111μm and 123μm for the three wires.

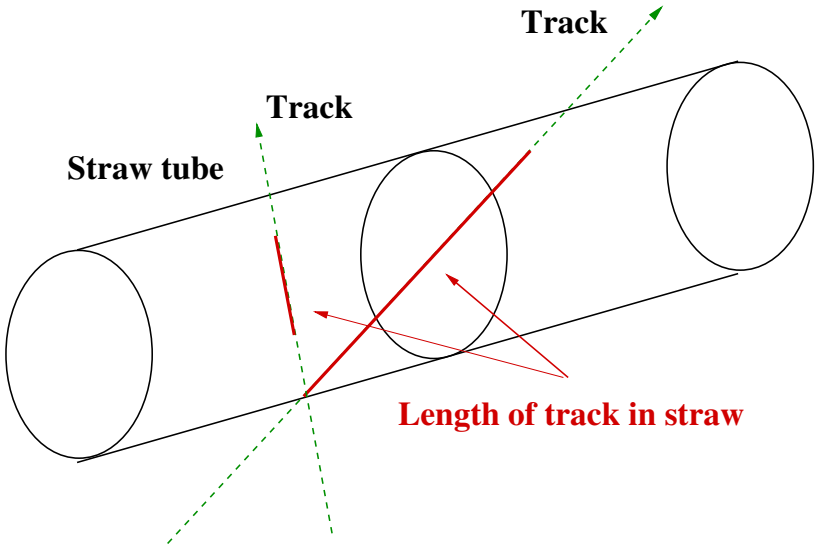

Figure 32: A schematic drawing of two tracks passing through a straw tube with quite different lengths inside the straw. In order to be able to utilize dE/dx information in the CDC, it is necessary to accurately compute the length of a track in a given straw tube.

Our studies will use cosmic tracks that cross roughly 90° from the length of the wire. The track fit to several tubes will then allow us to compute the track length in a given straw tube, and thus computing the relevant dx. The energy deposit can then be computed by analytically summing the charge in a given pulse. To first order, this is simply a sum of all channels above pedestal from where the signal starts until it falls back close to pedestal.

For cosmics, we will then assume that all particles are minimum ionizing $\mu^{\pm}$, which should then produce (roughly) the same dE/dx. Looking at the spread in this for a large number of tracks will allow us to set limits on how well this measurement can be performed.

12.5 Future Activities

Given that we are still a bit less than a year away from the proposed start of construction of the 12 GeV upgrade, we anticipate utilizing the time to continue to study the current prototype and also to work on a new, smaller prototype to refine some of the constructions techniques that were originally developed six years ago.

With regard to the studies of the current prototype chamber, we anticipate extending the current work to include tracks crossing the chamber at a wide range of angles. This can be carried out by using our existing cosmic trigger, but tilting the chamber to a set of predefined angles.

We also plan to look in detail at the energy-loss information for cosmics—mostly with the goal of understanding the correct track-length and angle corrections. With cosmics, we would need to assume that all particles are minimum ionizing. However, given that the path length in the straws will be different, the energy deposited should scale with that length and we should be able to see it.

In an attempt to add additional z position information beyond what is obtained with the stereo layers, it may be possible to gang together pairs of wires at the downstream end of the chamber. There would then effectively be a readout at each end of the wire and one could use charge division to determine the position along the wire. A decision to proceed along this route will not affect the overall cost or schedule of the chamber and will be based on planned studies with the prototype. If it is possible to measure z at the $\approx 10\,cm$ level for each hit, this could greatly facilitate pattern recognition in the chamber.

In addition to the work with the current chamber, we would like to build a small chamber that could easily be transported for either beam or magnet tests. This would use as much of the final parts as possible (all machined in house). In addition to being useful in working with the final chamber parts, it will also help us transfer some hands-on information from current very senior graduate students to the people that are likely to build the final chamber.

13 List of Design Parameters

Table 7: CDC Geometry

Active volume inner radius:	10.18 cm
Active volume outer radius:	55.42 cm
Active length:	150 cm
Chamber assembly outer radius:	60.0 cm
Axial layers (1-3):	10.16 to 15.32 cm
Stereo layers (4-7):	15.5 to 22.45 cm
Axial layers (8-12):	23.9 to 32.63 cm
Stereo layers (13-16):	32.81 to 39.76 cm
Axial layers (17-24):	40.81 to 55.42 cm
Thickness per layer (g/cm2):	0.051
Thickness per layer (rad. lengths):	0.0014
Thickness per 24 layers (rad. lengths):	0.035

Table 8: CDC Materials

Gas (at 1 at.):	Ar/CO_2 87/13
Gas (at 1 at.):	$Ar/CO_2/CH_4$ 80/10/10 (possibly)
Number of cables : (50-conductor shielded ribbon cables)	3098/24 = 130
Positioning accuracy of sense wires (x,y):	40 μm
Positioning accuracy of package (z):	0.5 mm
Thickness of inner shell (g/cm2):	0.162
Thickness of inner shell (rad. lengths):	0.0067
Thickness of outer shell (g/cm2):	0.2 cm of aluminum
Thickness of outer shell (rad. lengths):	0.031
Strawtube (diameter):	1.6 cm
Strawtube (material):	Aluminized Kapton
Strawtube (thickness):	100(5) μm Kapton(Al)
Number of sense wires (20 micron gold-plated W):	3098
Upstream Endplate:	0.9525 cm Al (3/8 plate)
Downstream Endplate:	0.6 cm Carbon Fiber
Upstream Feedthrus:	Al
Downstream Feedthrus:	Delrin
Plenums:	Plexiglas
Wire Tension:	$\approx$ 37g ($\frac{1}{2}$ of yield point).

Table 9: Location of CDC active areas

Upstream gas plenum:	$-3\,cm$
Upstream active volume:	$17\,cm$
Downstream active volume:	$167\,cm$
Downstream gas plenum:	$177\,cm$

Table 10: CDC dE/dx capability

Sense wires:	YES
Momentum Range:	$p \leq 450 MeV/c$

Table 11: Operating Parameters:

Nominal operating voltage (sense):	$+1800\,V$
Nominal gas gain:	5×10^4
Gas flow:	5 chamber volumes/day

Table 12: Preamplifier and readout parameters

Gain of prototype:	$3.6 mv/fC$
Noise level:	$3000\,e$ RMS at 20pF
Peaking time:	$\sim 11\,ns$
Tail compensation:	YES
Cable length to post-amp:	$13\,m$
Discriminator output:	NO
Readout:	$125\,MHz$ FADCs

Table 13: CDC Calibration and resolution

Sense wires (selected charge):	electronic pulser
Perpendicular to wire (σ):	$\approx 150\,\mu m$
z-position from stereo (σ):	$\approx 1.5\,mm$

References

[1] Rob Veenhof, **The GARFIELD Program, Simulation of Gaseous Detectors**", `http://garfield.web.cern.ch/garfield/`, (1984).

[2] A. Dzierba *et al.* **Physics and Detector Performance Metrics** GlueX Document 865, February 2008.

[3] H. Wirth, *et al.* (The JETSET Collaboration), **Particle Identification with the JETSET Straw Chambers**, Nucl. Instrum. Methods A**367**, 248, (1995).

[4] Zebulun Krahn and Curtis A. Meyer, **Gas Composition Study for the Straw Tube Chamber in the GlueX Detector at Jefferson Lab**, GlueX Document 62, November 2002.

[5] Curtis A. Meyer, **A Study of Vertex Resolution in GlueX**, GlueX Document 388, November 2004.

[6] Fernando Barbosa, **GlueX Preamp Card User's Manual**, GlueX Document 923, December 2007.

[7] Dan Carman, **FDC On-Chamber Electronics**, GlueX Document 753, February 2007.

[8] Curtis A. Meyer, **Budget Justification for the GlueX Central Drift Chamber**, GlueX Document 764, July 2007.

[9] Fernando Barbosa, **Low Voltage Distribution for the Hall D CDC and FDC Detectors** GlueX Document 966, January 2008.

[10] Fernando Barbosa, **High Voltage Distribution for the Hall D CDC and FDC Detectors** GlueX Document 967, February 2008.

[11] H.Baerwolff, *et. al*, **Design and performance of a full scale prototype of the outer z-drift chamber for the H1 experiment at HERA**, Zeuthen Document PHE-89-02, Desy 89-3-105 (1988).

[12] V. Commichau, *et. al*, **Test of a High Resolution Drift Chamber Prototype**, Nucl. Instrum. Methods A**235**, 267, (1985).